NASA / TM—2004-212328

Fracture Mechanics Analysis of an Annular Crack in a Three-Concentric-Cylinder Composite Model

Latife H. Kuguoglu
QSS Group, Inc., Cleveland, Ohio

Wieslaw K. Binienda
University of Akron, Akron, Ohio

Gary D. Roberts
Glenn Research Center, Cleveland, Ohio

February 2004

The NASA STI Program Office . . . in Profile

Since its founding, NASA has been dedicated to the advancement of aeronautics and space science. The NASA Scientific and Technical Information (STI) Program Office plays a key part in helping NASA maintain this important role.

The NASA STI Program Office is operated by Langley Research Center, the Lead Center for NASA's scientific and technical information. The NASA STI Program Office provides access to the NASA STI Database, the largest collection of aeronautical and space science STI in the world. The Program Office is also NASA's institutional mechanism for disseminating the results of its research and development activities. These results are published by NASA in the NASA STI Report Series, which includes the following report types:

- TECHNICAL PUBLICATION. Reports of completed research or a major significant phase of research that present the results of NASA programs and include extensive data or theoretical analysis. Includes compilations of significant scientific and technical data and information deemed to be of continuing reference value. NASA's counterpart of peer-reviewed formal professional papers but has less stringent limitations on manuscript length and extent of graphic presentations.

- TECHNICAL MEMORANDUM. Scientific and technical findings that are preliminary or of specialized interest, e.g., quick release reports, working papers, and bibliographies that contain minimal annotation. Does not contain extensive analysis.

- CONTRACTOR REPORT. Scientific and technical findings by NASA-sponsored contractors and grantees.

- CONFERENCE PUBLICATION. Collected papers from scientific and technical conferences, symposia, seminars, or other meetings sponsored or cosponsored by NASA.

- SPECIAL PUBLICATION. Scientific, technical, or historical information from NASA programs, projects, and missions, often concerned with subjects having substantial public interest.

- TECHNICAL TRANSLATION. English-language translations of foreign scientific and technical material pertinent to NASA's mission.

Specialized services that complement the STI Program Office's diverse offerings include creating custom thesauri, building customized databases, organizing and publishing research results . . . even providing videos.

For more information about the NASA STI Program Office, see the following:

- Access the NASA STI Program Home Page at ***http://www.sti.nasa.gov***

- E-mail your question via the Internet to help@sti.nasa.gov

- Fax your question to the NASA Access Help Desk at 301–621–0134

- Telephone the NASA Access Help Desk at 301–621–0390

- Write to:
  NASA Access Help Desk
  NASA Center for AeroSpace Information
  7121 Standard Drive
  Hanover, MD 21076

NASA / TM—2004-212328

Fracture Mechanics Analysis of an Annular Crack in a Three-Concentric-Cylinder Composite Model

Latife H. Kuguoglu
QSS Group, Inc., Cleveland, Ohio

Wieslaw K. Binienda
University of Akron, Akron, Ohio

Gary D. Roberts
Glenn Research Center, Cleveland, Ohio

National Aeronautics and
Space Administration

Glenn Research Center

February 2004

Acknowledgments

This work was supported in part by NASA Glenn Research Center through grants NAG3–1223 and NCC3–744.

This work was sponsored by the Low Emissions Alternative Power Project of the Vehicle Systems Program at the NASA Glenn Research Center.

Available from

NASA Center for Aerospace Information
7121 Standard Drive
Hanover, MD 21076

National Technical Information Service
5285 Port Royal Road
Springfield, VA 22100

Available electronically at http://gltrs.grc.nasa.gov

Table of Contents

Fracture Mechanics Analysis of an Annular Crack in a Three-Concentric-Cylinder Composite Model

Latife H. Kuguoglu
QSS Group, Inc.
Cleveland, Ohio 44135

Wieslaw K. Binienda
University of Akron
Akron, Ohio 44325–3905

Gary D. Roberts
National Aeronautics and Space Administration
Glenn Research Center
Cleveland, Ohio 44135

Summary

A boundary-value problem governing a three-phase concentric-cylinder model was analytically modeled to analyze annular interfacial crack problems with Love's strain functions in order to find the stress intensity factors (SIFs) and strain energy release rates (SERRs) at the tips of an interface crack in a nonhomogeneous medium. The complex form of a singular integral equation (SIE) of the second kind was formulated using Bessel's functions in the Fourier domain, and the SIF and total SERR were calculated using Jacoby polynomials. For the validity of the SIF equations to be established, the SIE of the three-concentric-cylinder model was reduced to the SIE for a two-concentric-cylinder model, and the results were compared with the previous results of Erdogan. A preliminary set of parametric studies was carried out to show the effect of interphase properties on the SERR. The method presented here provides insight about the effect of interphase properties on the crack driving force.

Introduction

Advanced composite materials are now being used widely for aerospace applications, and the development of reliable analysis methods for these composite structures has contributed to the growing use of composite materials. Methods for analyzing the deformation of a composite structure under load are well established. However, methods for analyzing strength and the degradation of strength during service are less developed. The initial strength of an undamaged composite can be analyzed using lamination theory and macroscopic failure criteria applied at the ply level. The effect of constituent properties can be included in the analysis using micromechanics. However, it is difficult to account for the initial presence of microscopic flaws and the growth of microscopic damage during service. For polymer matrix composites, the initial presence and growth of flaws in the region of the fiber-matrix interface have a large effect on strength retention. Development of reliable models for the growth of damage in this interfacial region would contribute to better understanding of the long-term durability of composite structures. Anisotropic and/or nonhomogeneous theories can describe the average macroscopic effect of microscopic damage such as fiber breaking, matrix cracking, and interface debonding. However, a fracture mechanics approach applied at the microscopic level is needed to account for the initiation and growth of microscopic damage. After microscopic damage has grown into a macroscopic defectlike interply delamination, failure can be analyzed from a macromechanics level (ref. 1).

On atomic and molecular scales, damage is treated differently in metals, ceramics, and polymers because of the inherent differences in the basic microstructures (ref. 2). In fracture mechanics, the driving force for the initiation and growth of damage is the strain energy release rate (SERR). The mathematical methods used to calculate the SERR for damage growth in a composite are the same for different types of

materials. However, the magnitude of the SERR and the critical SERR for the growth of damage depend on material properties and molecular damage processes.

In the present work, the fracture mechanics problem of a crack in the interfacial region of a composite is studied. Although the model could be used for analyzing metal and ceramic matrix composites, in this report the model is applied to polymer matrix composites. In a simplified view, a polymer matrix composite is composed of two materials (fiber and matrix) with different but uniform properties separated by a planar interface. In reality, there is often a region of finite thickness near the interface with properties different from the fiber or the matrix. This region is sometimes introduced intentionally. For example, a sizing is often applied to fibers to improve weaving characteristics and to improve adhesion between the fiber and matrix in the cured composite. Although the sizing material is chemically compatible with the matrix material, the mechanical properties of the sizing and matrix are not necessarily equal. Another reason for the presence of a third region between the fiber and matrix is the effect of the interface on the formation of the matrix material during composite fabrication. For thermoplastic matrix materials, the degree of crystallinity near the fiber can be different from that in the bulk region. For thermosetting matrix materials, the presence of the fiber surface affects the cure reactions so that the chemical structure of the matrix material is different near the fiber. The region of finite thickness between the fiber and matrix is called the interphase. The thickness and properties of the interphase depend on the particular combination of fiber, sizing, and matrix used as well as the composite processing conditions. Other researchers have attempted to model variations in material composition and properties in the interphase region of a composite material (refs. 3 and 4). This report does not investigate a specific material system. Instead, the fracture mechanics model developed in this report is used for a parametric analysis of the effect of interphase thickness and stiffness on the stress intensity factor (SIF) and SERR.

A fracture mechanics analysis of an interface crack in a three-component system (fiber, matrix, and interphase) is performed within the confines of the linear theory of elasticity. The crack problem is of the mixed boundary value type and is reduced to a system of singular integral equations (SIEs). Except under very special circumstances where a closed-form solution can be found (ref. 5), systems of SIEs are solved by a numerical method to obtain the crack-tip SIF and SERR. The SIF and SERR are the forces driving damage growth and are related to the effects of applied loads, crack geometry, and material properties. The goals of this work are to obtain solutions for crack-tip SIF and SERR and to use these solutions to evaluate the effects of material properties and interphase thickness on damage propagation.

A brief description of the formulation of the problem follows. The first step is to develop some basic forms capable of modeling a cylindrical fiber. The cylindrical coordinates r, θ, and x are used. The variable x is used instead of the more common z in order to be consistent with reference 5. Results from this report reduce to those in reference 5 under special circumstances. In the boundary value problem considered, there is a coating between a straight elastic fiber of finite radius and an infinite elastic matrix material of different thermomechanical properties. The coating could be the interphase in a polymer matrix composite or, more generally, any coating in any composite material. The bonding between the fiber and the coating is assumed to be perfect. The bonding between the coating and matrix is perfect, but there are axially symmetric cracks on the coating-matrix interface. The applied external loads cause traction on the surfaces of the cracks. The goals are to obtain a solution for crack-tip singularities, to find the stress distribution in the medium, and to find the energy release rates for the propagation of the crack along the interface.

A special case with only two cracks extending to infinity along the axial direction is shown in figure 1. An infinitely long straight fiber and matrix material extending to infinity both axially and radially are joined by a third material called the coating. The bonding between the fiber and the coating is perfect. The bonding between the coating and the matrix is perfect in the centered region of contact. In figure 1, r is the radial direction, x is the axial direction, and (μ_1, ν_1), (μ_2, ν_2), and (μ_3, ν_3) are the elastic constants of the matrix, fiber, and coating, respectively. There is a geometric symmetry in the medium with respect to the $x = 0$ plane. The fiber radius r_f is finite, the radius of the coating r_c is finite, and the radius of the matrix r_m is infinitely large.

To solve the elasticity problem for the geometry shown in figure 1, first the Green's function for each layer is obtained. Using stress and displacement equations and boundary conditions on the interface of the coating and matrix, the integral equations of the problem are derived. These integral equations are reduced to a system of SIEs.

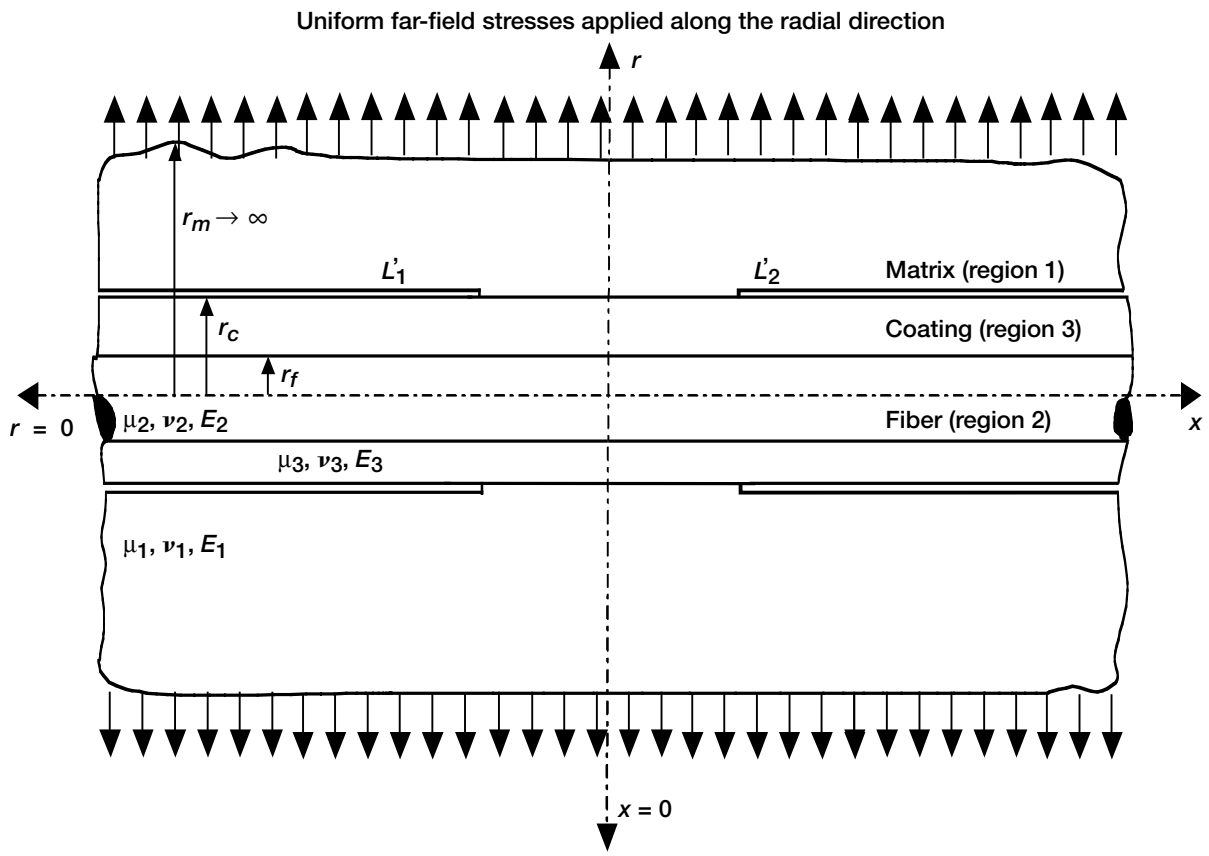

Figure 1.—Three-concentric-cylinder model with interface annular cracks. L, length of the bonded interface; L'_1, L'_2, length of the debonded interfaces; E_1, E_2, E_3, modulus of elasticity for the matrix, fiber, and coating; r_m, radius of the matrix; r_f, radius of the fiber; r_c, radius of the coating; ν_1, ν_2, ν_3, Poisson ratios for the matrix, fiber, and coating; μ_1, μ_2, μ_3, elastic constants of the matrix, fiber, and coating.

Analytical Solution

Governing Equations

This investigation deals with the plane strain problem (or the generalized plane stress in which the mean state of stress across the thickness is considered, or the quasi-plane state of stress in which the θ variable is ignored) for bonded materials. The problem considered here is axisymmetric. There is an existing geometric symmetry about the $x = 0$ plane. The external loads are separated into symmetric and antisymmetric components with respect to the $x = 0$ plane, and the only nonzero stress and displacement components in an infinitely long cylindrical domain are given by equations (1) to (6) (refs. 5 to 7). In these equations, t is a dummy variable of the Fourier domain, F is the Love strain function, ν is the Poisson's ratio, and r is the radial distance.

$$\sigma_r(r,x) = \frac{2}{\pi}\int_0^\infty \left(\nu\nabla^2 - \frac{d^2}{dr^2}\right) F \begin{pmatrix} \cos(xt) \\ -\sin(xt) \end{pmatrix} tdt \tag{1}$$

$$\sigma_\theta(r,x)=\frac{2}{\pi}\int_0^\infty\left(\nu\nabla^2-\frac{1}{r}\frac{d}{dr}\right)F\begin{pmatrix}\cos(xt)\\-\sin(xt)\end{pmatrix}tdt \tag{2}$$

$$\sigma_x(r,x)=\frac{2}{\pi}\int_0^\infty\left[(2-\nu)\nabla^2+t^2\right]F\begin{pmatrix}\cos(xt)\\-\sin(xt)\end{pmatrix}tdt \tag{3}$$

$$\tau_{rx}(r,x)=\frac{2}{\pi}\int_0^\infty\frac{d}{dr}\left[(1-\nu)\nabla^2+t^2\right]F\begin{pmatrix}\sin(xt)\\\cos(xt)\end{pmatrix}dt \tag{4}$$

$$u_r(r,x)=\frac{1}{\pi\mu}\int_0^\infty\frac{dF}{dr}\begin{pmatrix}-\cos(xt)\\\sin(xt)\end{pmatrix}tdt \tag{5}$$

$$u_x(r,x)=\frac{1}{\pi\mu}\int_0^\infty\left[(1-2\nu)\nabla^2+\frac{d^2}{dr^2}+\frac{1}{r}\frac{d}{dr}\right]F\begin{pmatrix}\sin(xt)\\\cos(xt)\end{pmatrix}dt \tag{6}$$

Because of existing boundary conditions and the plane strain assumption with no torsional stresses, it is convenient to use the Love strain function F to develop the solution following a procedure similar to that in reference 5. The Love strain function F can also be called the Green's function. In the absence of body forces, F is defined by the following biharmonic equation in cylindrical coordinates:

$$\nabla^2\nabla^2F(r,t)=0 \tag{7}$$

where the Laplacian operator in cylindrical coordinates is

$$\nabla^2=\frac{d^2}{dr^2}+\frac{1}{r}\frac{d}{dr}-t^2 \tag{8}$$

The solution of equation (7) is as follows, where $\rho = rt$

$$F(r,t)=AK_0(\rho)+B\rho K_1(\rho)+CI_0(\rho)+D\rho I_1(\rho) \tag{9}$$

The Green's functions $F(r, t)$ for each layer are

$$F_1(r,t)=A_1K_0(\rho)+B_1\rho K_1(\rho)+C_1I_0(\rho)+D_1\rho I_1(\rho)\qquad r_ct<\rho<\infty \tag{10}$$

$$F_2(r,t)=A_2K_0(\rho)+B_2\rho K_1(\rho)+C_2I_0(\rho)+D_2\rho I_1(\rho)\qquad 0<\rho<r_ft \tag{11}$$

$$F_3(r,t)=A_3K_0(\rho)+B_3\rho K_1(\rho)+C_3I_0(\rho)+D_3\rho I_1(\rho)\qquad r_ft<\rho<r_ct \tag{12}$$

where A_1, B_1, C_1, D_1, A_2, B_2, C_2, D_2, A_3, B_3, C_3, and D_3 are the unknown constants that are functions of the transform variable t.

So that the solution will be bonded for the first and second layer (matrix and fiber) and because of the behavior of the Bessel functions at $r = \infty$ and $r = 0$, some of the constants become zero. For the matrix, $C_1 = 0$ and $D_1 = 0$. For the fiber, $A_2 = 0$ and $B_2 = 0$. Therefore, the solutions for the unknown Green's functions of each layer become

$$F_1(r,t) = A_1(t)K_0(\rho) + B_1(t)\rho K_1(\rho) \tag{13}$$

$$F_2(r,t) = C_2(t)I_0(\rho) + D_2(t)I_1(\rho) \tag{14}$$

$$F_3(r,t) = A_3(t)K_0(\rho) + B_3(t)K_1(\rho) + C_3(t)I_0(\rho) + D_3(t)I_1(\rho) \tag{15}$$

The functions F_1, F_2, and F_3, and their derivatives, are substituted into the stress and displacement equations (1) to (6), where $\rho = rt$, $r_c \le r_1 \le \infty$, $0 \le r_2 \le r_f$, $r_f \le r_3 \le r_c$, r_f is the radius of the fiber, and r_c is the radius of the coating.

The continuity of the radial stresses (eqs. (1) to (3)), the shear stress equation (eq. (4)), the radial displacement equation (eq. (5)), and the axial displacement equation (eq. (6)) at the matrix-coating interface and the fiber-coating interface must be applied to find the unknown constants A_3, B_3, C_3, D_3, A_1, B_1, A_2, and B_2. Using $r_3 = r_1 = r_c$ at the matrix-coating interface and defining $\alpha = r_c t$ transforms equations (1), (4), (5), and (6) into equations (16) to (23):

$$\sigma_{r1}(r_c, x) = \frac{2}{\pi}\int_0^\infty t^3\left[-A_1K_0(\alpha) - \frac{A_1}{\alpha}K_1(\alpha) + (1-2\nu_1)B_1K_0(\alpha) - B_1\alpha K_1(\alpha)\right]\cos(xt)dt \tag{16}$$

$$\sigma_{r3}(r_c, x) = \frac{2}{\pi}\int_0^\infty t^3\left[\begin{array}{l} A_3\left(-K_0(\alpha) - \frac{1}{\alpha}K_1(\alpha)\right) + B_3\begin{pmatrix}(1-2\nu_3)K_0(\alpha)\\ -\alpha K_1(\alpha)\end{pmatrix} \\ \quad + C_3\left(-I_0(\alpha) + \frac{1}{\alpha}I_1(\alpha)\right) + D_3\begin{pmatrix}(2\nu_3-1)I_0(\alpha)\\ -\alpha I_1(\alpha)\end{pmatrix}\end{array}\right]\cos(xt)dt \tag{17}$$

$$\tau_{rx1}(r_c, x) = \frac{2}{\pi}\int_0^\infty t^3\left[-A_1K_1(\alpha) + 2B_1K_1(\alpha) - B_1\alpha K_0(\alpha) - 2\nu_1B_1K_1(\alpha)\right]\sin(x)dt \tag{18}$$

$$\tau_{rx3}(r_c, x) = \frac{2}{\pi}\int_0^\infty t^3\left[\begin{array}{l} -A_3K_1(\alpha) + B_3\left(2K_1(\alpha) - \alpha K_0(\alpha) - 2\nu_3K_1(\alpha)\right) \\ \quad + C_3I_1(\alpha) + D_3(2(1-\nu_3)I_1(\alpha) + \alpha I_0(\alpha))\end{array}\right]\sin(xt)dt \tag{19}$$

$$u_{r1}(r_c, x) = -\frac{1}{\pi\mu_1}\int_0^\infty t^2\left[-A_1K_1(\alpha) - B_1\alpha K_0(\alpha)\right]\cos(xt)dt \tag{20}$$

$$u_{r3}(r_c, x) = -\frac{1}{\pi\mu_3}\int_0^\infty t^2\left[-A_3K_1(\alpha) - B_3\alpha K_0(\alpha) + C_3I_1(\alpha) + D_3\alpha I_0(\alpha)\right]\cos(xt)dt \tag{21}$$

$$u_{x1}(r_c, x) = \frac{1}{\pi\mu_1}\int_0^\infty t^2\left[A_1K_0(\alpha) + B_1(\alpha K_1(\alpha) - 4(1-\nu_1)K_0(\alpha)\right]\sin(xt)dt \tag{22}$$

$$u_{x3}(r_c, x) = \frac{1}{\pi\mu_3}\int_0^\infty t^2\left\{\begin{array}{l} A_3K_0(\alpha) + B_3\left[\alpha K_1(\alpha) - 4(1-\nu_3)K_0(\alpha)\right] \\ \quad + C_3I_0(\alpha) + D_3\left[\alpha I_1(\alpha) + 4(1-\nu_3)I_0(\alpha)\right]\end{array}\right\}\sin(xt)dt \tag{23}$$

Using $r_3 = r_2 = r_f$ at the fiber-coating interface and defining $\gamma = r_f\, t$ transforms equations (1), (4), (5), and (6) into equations (24) to (31):

$$\sigma_{r2}(r_f, x) = \frac{2}{\pi}\int_0^\infty t^3 \left\{ C_3\left[-I_0(\gamma) + \frac{1}{\alpha} I_1(\gamma)\right] + D_3\left[(2\nu_3 - 1)I_0(\gamma) - \gamma I_1(\gamma)\right]\right\} \cos(xt)\,dt \tag{24}$$

$$\sigma_{r3}(r_f, x) = \frac{2}{\pi}\int_0^\infty t^3 \left\{ \begin{array}{l} A_3\left[-K_0(\gamma) - \dfrac{1}{\gamma} K_1(\gamma)\right] + B_3\left[(1-2\nu_3)K_0(\gamma) - \gamma K_1(\gamma)\right] \\ \quad + C_3\left[-I_0(\gamma) + \dfrac{1}{\gamma} I_1(\gamma)\right] + D_3\left[(2\nu_3 - 1)I_0(\gamma) - \alpha I_1(\gamma)\right] \end{array} \right\} \cos(xt)\,dt \tag{25}$$

$$\tau_{rx2}(r_f, x) = \frac{2}{\pi}\int_0^\infty t^3 \left\{ C_2 I_1(\gamma) + D_2\left[2(1-\nu_2) I_1(\gamma) + \gamma I_0(\gamma)\right]\right\} \sin(xt)\,dt \tag{26}$$

$$\tau_{rx3}(r_f, x) = \frac{2}{\pi}\int_0^\infty t^3 \left\{ \begin{array}{l} -A_3 K_1(\gamma) + B_3\left[2K_1(\gamma) - \gamma K_0(\gamma) - 2\nu_3 K_1(\gamma)\right] \\ \quad + C_3 I_1(\gamma) + D_3\left[2(1-\nu_3) I_1(\gamma) + \alpha I_0(\gamma)\right] \end{array} \right\} \sin(xt)\,dt \tag{27}$$

$$u_{r2}(r_f, x) = -\frac{1}{\pi\mu_2}\int_0^\infty t^2 \left[C_2 I_1(\gamma) + D_2 \gamma I_0(\gamma)\right] \cos(xt)\,dt \tag{28}$$

$$u_{r3}(r_f, x) = -\frac{1}{\pi\mu_3}\int_0^\infty t^2 \left[-A_3 K_1(\gamma) - B_3\,\gamma K_0(\gamma) + C_3 I_1(\gamma) + D_3 \gamma I_0(\gamma)\right] \cos(xt)\,dt \tag{29}$$

$$u_{x2}\left(r_f, x\right) = \frac{1}{\pi\mu_2}\int_0^\infty t^2 \left\{ C_2 I_0\left(\gamma\right) + D_2\left[\gamma I_1\left(\gamma\right) + 4\left(1-\nu_2\right) I_0\left(\gamma\right)\right]\right\} \sin\left(xt\right)dt \tag{30}$$

$$u_{x3}\left(r_f, x\right) = \frac{1}{\pi\mu_3}\int_0^\infty t^2 \left\{ \begin{array}{l} A_3 K_0(\gamma) + B_3\left[\gamma K_1(\gamma) - 4(1-\nu_3) K_0(\gamma)\right] \\ \quad + C_3 I_0\left(\gamma\right) + D_3\left[\gamma I_1\left(\gamma\right) + 4\left(1-\nu_3\right) I_0\left(\gamma\right)\right] \end{array} \right\} \sin\left(xt\right)dt \tag{31}$$

Boundary Conditions

Thermomechanical stresses in the medium without the crack are assumed to be known since they can be easily calculated. Hence, by simple superposition, the original problem (fig. 2) can be reduced to one in which external loads are first applied to a system with the coating-matrix completely separated (fig. 3) and perturbation loads are then applied to close the crack in the bonded region (fig. 4).

The stress-related boundary conditions at the matrix-coating (region 1 to region 3) interface, where $r_1 = r_3 = r_c$ are

$$\sigma_{r1}\left(r_c, x\right) = \sigma_{r3}(r_c, x) = p\delta\left(x - \xi\right) \pm p\delta\left(x + \xi\right) \tag{32}$$

and

$$\tau_{rx1}\left(r_c, x\right) = \tau_{rx3}\left(r_c, x\right) = q\delta\left(x - \xi\right) \pm q\delta\left(x + \xi\right) \tag{33}$$

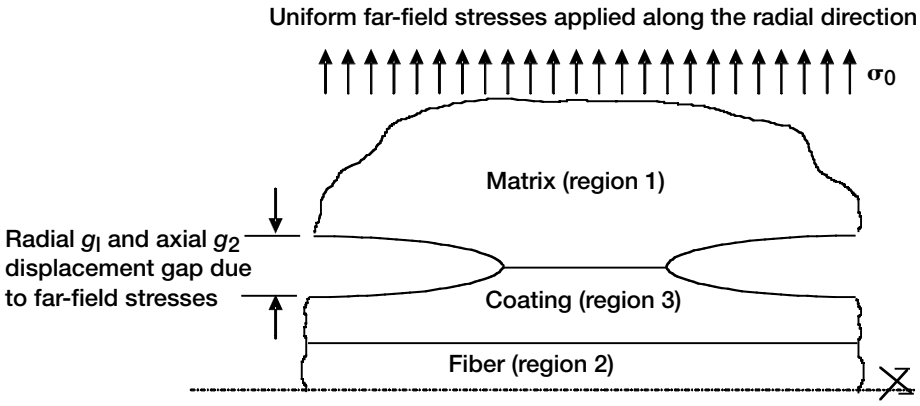

Figure 2.—Original problem.

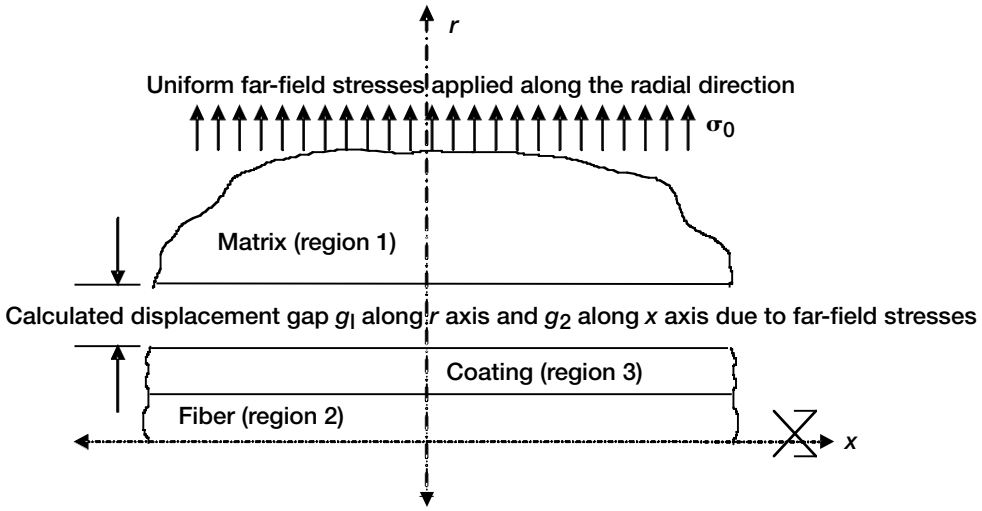

Figure 3.—Elasticity problem—far-field stress applied with no bonding at the coating-matrix interface and a gap equal to the calculated displacements g_1 along the radial axis and g_2 along the axial axis in figure 2.

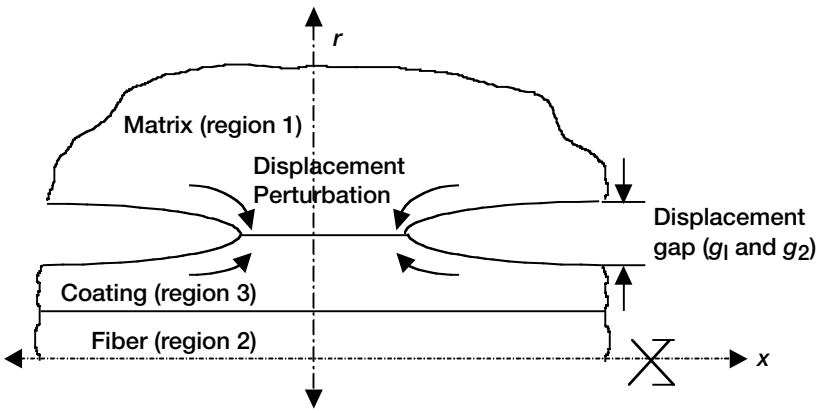

Figure 4.—Mixed boundary value problem—the unbonded problem of figure 3 with a displacement perturbation to close the crack in the bonded region.

where p and q are the unknown stresses outside the crack. The p and q stresses are zero along the crack surface. The displacement-related boundaries at the matrix-coating (region1 to region 3) interface are

$$u_{r1}(r_c, x) - u_{r3}(r_c, x) = g_1\delta(x-\xi) \pm g_1\delta(x+\xi) \tag{34}$$

and

$$u_{x1}(r_c, x) - u_{x3}(r_c, x) = g_2\delta(x-\xi) \pm g_2\delta(x+\xi) \tag{35}$$

where g_1 and g_2 are known radial and axial distances between the inner diameter of the matrix cylinder and the outer diameter of the coating cylinder while these cylinders are completely separated.

Both stress and displacement boundary conditions are applied at the fiber-coating (region 2 to region 3) interface because there is no debonding. The boundary conditions at the fiber-coating interface, where $r_2 = r_3 = r_f$, are given in equations (36) to (39):

$$\sigma_{r2}(r_f, x) = \sigma_{r3}(r_f, x) \tag{36}$$

$$\tau_{rx2}(r_f, x) = \tau_{rx3}(r_f, x) \tag{37}$$

$$u_{r2}(r_f, x) = u_{r3}(r_f, x) \tag{38}$$

$$u_{x2}(r_f, x) = u_{x3}(r_f, x) \tag{39}$$

Green's Function

There are eight unknown constants and eight equations at the matrix-coating (region 1 to region 3) and fiber-coating (region 2 to region 3) interfaces. Substituting equations (16) and (18) into equations (32) and (33) establishes the following two equations with two unknowns:

$$\frac{2}{\pi}\int_0^\infty t^3 \left[\begin{array}{l} -A_1K_0(\alpha) - \dfrac{A_1}{\alpha}K_1(\alpha) \\ \qquad + (1-2\nu_1)B_1K_0(\alpha) - B_1\alpha K_1(\alpha) \end{array} \right] \cos(xt)dt = p(x)\delta(x-\xi) \tag{40}$$

and

$$\frac{2}{\pi}\int_0^\infty t^3 \left[\begin{array}{l} -A_1K_1(\alpha) + 2B_1K_1(\alpha) \\ \qquad - B_1\alpha K_0(\alpha) - 2\nu_1B_1K_1(\alpha) \end{array} \right] \sin(x)dt = q(x)\delta(x-\xi) \tag{41}$$

Making an inverse Fourier cosine transformation to equation (40) results in equation (42):

$$t^3 \left[\begin{array}{l} -A_1K_0(\alpha) - \dfrac{A_1}{\alpha}K_1(\alpha) \\ \qquad + (1-2\nu_1)B_1K_0(\alpha) - B_1\alpha K_1(\alpha) \end{array} \right] = \int_0^\infty p(x)\delta(x-\xi)\cos(xt)dx \tag{42}$$

Using the properties of the Dirac delta function changes equation (42) into equation (43):

$$t^3\left[-A_1K_0(\alpha)-\frac{A_1}{\alpha}K_1(\alpha)+(1-2\nu_1)B_1K_0(\alpha)-B_1\alpha K_1(\alpha)\right]=p(\xi)\cos(\xi t) \tag{43}$$

Applying an inverse Fourier sine transformation to equation (41) implies equation (44):

$$t^3\left[-A_1K_1(\alpha)+2B_1K_1(\alpha)-B_1\alpha K_0(\alpha)-2\nu_1B_1K_1(\alpha)\right]=\int_0^\infty q(x)\delta(x-\xi)\sin(xt)dx \tag{44}$$

Because of the properties of the Dirac delta function, equation (44) becomes equation (45):

$$t^3\left[-A_1K_1(\alpha)+2B_1K_1(\alpha)-B_1\alpha K_0(\alpha)-2\nu_1B_1K_1(\alpha)\right]=q(x)\sin(\xi t) \tag{45}$$

Equations (43) and (45) can be written in matrix form as equation (46) with A_1 and B_1 as unknowns:

$$\begin{bmatrix}-K_0(\alpha)-\dfrac{K_1(\alpha)}{\alpha} & (1-2\nu_1)K_0(\alpha)-\alpha K_1(\alpha)\\ -K_1(\alpha) & 2K_1(\alpha)-\alpha K_0(\alpha)-2\nu_1K_1(\alpha)\end{bmatrix}\begin{bmatrix}A_1(t)\\ B_1(t)\end{bmatrix}=\begin{bmatrix}\dfrac{p(\xi)}{t^3}\cos(\xi t)\\ \dfrac{q(\xi)}{t^3}\sin(\xi t)\end{bmatrix} \tag{46}$$

Solving equation (46) for A_1 and B_1 yields equations (47) and (48) with Δ_1 defined in equation (49):

$$A_1(t)=\frac{\alpha}{t^3\Delta_1}\left\{\begin{matrix}p(\xi)\cos(\xi t)\left[\alpha K_0(\alpha)-2(1-\nu_1)K_1(\alpha)\right]\\ +q(\xi)\sin(\xi t)\left[(1-2\nu_1)K_0(\alpha)-\alpha K_1(\alpha)\right]\end{matrix}\right\} \tag{47}$$

$$B_1(t)=\frac{\alpha}{t^3\Delta_1}\left\{\begin{matrix}-p(\xi)\cos(\xi t)\left[K_1(\alpha)\right]\\ +q(\xi)\sin(\xi t)\left[K_0(\alpha)-\dfrac{K_1(\alpha)}{\alpha}\right]\end{matrix}\right\} \tag{48}$$

$$\Delta_1=-\alpha^2K_0^{\,2}(\alpha)+\left[\alpha^2+2(1-\nu_1)\right]K_1^{\,2}(\alpha) \tag{49}$$

Equations (17), (19), and (24) to (29) are substituted into equations (32), (33), and (36) to (39), respectively, in order to find the other unknown constants—A_3, B_3, C_3, and D_3—at the matrix-coating (region 1 to region 3) interface and C_2, and D_2 at the fiber-coating (region 2 to region 3) interface. Using equation (17) in equation (32) results in the matrix form in equation (50):

$$\frac{2}{\pi}\int_0^\infty t^3\left\{\begin{matrix}A_3\left[-K_0(\alpha)-\dfrac{1}{\alpha}K_1(\alpha)\right]\\ +B_3\left[(1-2\nu_3)K_0(\alpha)-\alpha K_1(\alpha)\right]\\ +C_3\left[-I_0(\alpha)+\dfrac{1}{\alpha}I_1(\alpha)\right]\\ +D_3\left[(2\nu_3-1)I_0(\alpha)-\alpha I_1(\alpha)\right]\end{matrix}\right\}\cos(xt)dt=p(x)\delta(x-\xi) \tag{50}$$

Applying an inverse Fourier cosine transformation to equation (50) yields equation (51):

$$t^3\left\{\begin{array}{l} A_3\left[-K_0(\alpha)-\dfrac{1}{\alpha}K_1(\alpha)\right]+B_3\left[(1-2\nu_3)K_0(\alpha)-\alpha K_1(\alpha)\right] \\ \quad +C_3\left[-I_0(\alpha)+\dfrac{1}{\alpha}I_1(\alpha)\right]+D_3\left[(2\nu_3-1)I_0(\alpha)-\alpha I_1(\alpha)\right] \end{array}\right\}=\int_0^\infty p(x)\delta(x-\xi)\cos(xt)dx \qquad (51)$$

Using the properties of the Dirac delta function changes equation (51) into equation (52):

$$t^3\left\{\begin{array}{l} A_3\left[-K_0(\alpha)-\dfrac{1}{\alpha}K_1(\alpha)\right]+B_3\left[(1-2\nu_3)K_0(\alpha)-\alpha K_1(\alpha)\right] \\ \quad +C_3\left[-I_0(\alpha)+\dfrac{1}{\alpha}I_1(\alpha)\right]+D_3\left[(2\nu_3-1)I_0(\alpha)-\alpha I_1(\alpha)\right] \end{array}\right\}=p(\xi)\cos(\xi t) \qquad (52)$$

Using equation (19) in equation (33) gives equation (53):

$$\frac{2}{\pi}\int_0^\infty t^3\left\{\begin{array}{l} -A_3K_1(\alpha) \\ \quad +B_3\left[2K_1(\alpha)-\alpha K_0(\alpha)-2\nu_3K_1(\alpha)\right] \\ \quad +C_3I_1(\alpha) \\ \quad +D_3\left[2(1-\nu_3)I_1(\alpha)+\alpha I_0(\alpha)\right] \end{array}\right\}\sin(xt)dt=q(x)\delta(x-\xi) \qquad (53)$$

Applying an inverse Fourier sine transformation to equation (53) yields equation (54):

$$t^3\left\{\begin{array}{l} -A_3K_1(\alpha)+B_3\left[2K_1(\alpha)-\alpha K_0(\alpha)-2\nu_3K_1(\alpha)\right] \\ \quad +C_3I_1(\alpha)+D_3\left[2(1-\nu_3)I_1(\alpha)+\alpha I_0(\alpha)\right] \end{array}\right\}=\int_0^\infty q(x)\delta(x-\xi)\sin(xt)dx \qquad (54)$$

Because of the properties of the Dirac delta function, equation (54) becomes equation (55):

$$t^3\left\{\begin{array}{l} -A_3K_1(\alpha)+B_3\left[2K_1(\alpha)-\alpha K_0(\alpha)-2\nu_3K_1(\alpha)\right] \\ \quad +C_3I_1(\alpha)+D_3\left[2(1-\nu_3)I_1(\alpha)+\alpha I_0(\alpha)\right] \end{array}\right\}=q(\xi)\sin(\xi t) \qquad (55)$$

Using equations (24) and (25) in equation (36) gives equation (56):

$$\begin{aligned} A_3\left[-K_0(\gamma)-\frac{1}{\gamma}K_1(\gamma)\right]+B_3\left[(1-2\nu_3)K_0(\gamma)-\gamma K_1(\gamma)\right]+C_3\left[-I_0(\gamma)+\frac{1}{\gamma}I_1(\gamma)\right] \\ +D_3\left[(2\nu_3-1)I_0(\gamma)-\alpha I_1(\gamma)\right]=C_2\left[-I_0(\gamma)+\frac{1}{\alpha}I_1(\gamma)\right]+D_2\left[(2\nu_3-1)I_0(\gamma)-\gamma I_1(\gamma)\right] \end{aligned} \qquad (56)$$

Using equations (26) and (27) in equation (37) yields equation (57):

$$\begin{aligned} -A_3K_1(\gamma)+B_3\left[2K_1(\gamma)-\gamma K_0(\gamma)-2\nu_3K_1(\gamma)\right]+C_3I_1(\gamma) \\ +D_3\left[2(1-\nu_3)I_1(\gamma)+\alpha I_0(\gamma)\right]=C_2I_1(\gamma)+D_2\left[2(1-\nu_2)I_1(\gamma)+\gamma I_0(\gamma)\right] \end{aligned} \qquad (57)$$

Using equations (28) and (29) in equation (38) yields equation (58):

$$-A_3K_1(\gamma)-B_3\gamma K_0(\gamma)+C_3I_1(\gamma)+D_3\gamma I_0(\gamma)=C_2I_1(\gamma)+D_2\gamma I_0(\gamma) \tag{58}$$

Using equations (30) and (31) in equation (39) yields equation (59):

$$A_3K_0(\gamma)+B_3\left[\gamma K_1(\gamma)-4(1-\nu_3)K_0(\gamma)\right]+C_3I_0(\gamma) \\ +D_3\left[\gamma I_1(\gamma)+4(1-\nu_3)I_0(\gamma)\right]=C_2I_0(\gamma)+D_2\left[\gamma I_1(\gamma)+4(1-\nu_2)I_0(\gamma)\right] \tag{59}$$

From equations (56), (57), (58), and (59), the matrix system in equation (60) is established, with $R1$, $R2$, $R3$, and $R4$ detailed in equations (61) to (64):

$$\begin{bmatrix} \begin{pmatrix} -K_0(\gamma) \\ -\frac{1}{\gamma}K_1(\gamma) \end{pmatrix} & \begin{pmatrix} (1-2\nu_3)K_0(\gamma) \\ -\gamma K_1(\gamma) \end{pmatrix} & \begin{pmatrix} -I_0(\gamma) \\ +\frac{1}{\gamma}I_1(\gamma) \end{pmatrix} & \begin{pmatrix} (2\nu_3-1)I_0(\gamma) \\ -\gamma I_1(\gamma) \end{pmatrix} \\ -K_1(\gamma) & \begin{pmatrix} 2K_1(\gamma) \\ -\gamma K_0(\gamma) \\ -2\nu_3K_1(\gamma) \end{pmatrix} & I_1(\gamma) & \begin{pmatrix} 2I_1(\gamma) \\ +\gamma I_0(\gamma) \\ -2\nu_3I_1(\gamma) \end{pmatrix} \\ K_1(\gamma) & \gamma K_0(\gamma) & -I_1(\gamma) & -\gamma I_0(\gamma) \\ K_0(\gamma) & \begin{pmatrix} \gamma K_1(\gamma) \\ -4(1-\nu_3)K_0(\gamma) \end{pmatrix} & I_0(\gamma) & \begin{pmatrix} \gamma I_1(\gamma) \\ +4(1-\nu_3)I_0(\gamma) \end{pmatrix} \end{bmatrix} \begin{bmatrix} A_3(t) \\ B_3(t) \\ C_3(t) \\ D_3(t) \end{bmatrix} = \begin{bmatrix} R1 \\ R2 \\ R3 \\ R4 \end{bmatrix} \tag{60}$$

where

$$R1=C_2\left[-I_0(\gamma)+\frac{1}{\alpha}I_1(\gamma)\right]+D_2\left[(2\nu_3-1)I_0(\gamma)-\gamma I_1(\gamma)\right] \tag{61}$$

$$R2=C_2I_1(\gamma)+D_2\left[2(1-\nu_2)I_1(\gamma)+\gamma I_0(\gamma)\right] \tag{62}$$

$$R3=C_2I_1(\gamma)+D_2\gamma I_0(\gamma) \tag{63}$$

$$R4=C_2I_0(\gamma)+D_2\left[\gamma I_1(\gamma)+4(1-\nu_2)I_0(\gamma)\right] \tag{64}$$

The solution of equation (60) yields equations (65) to (68) for the unknown constants A_3, B_3, C_3, and D_3 in terms of C_2 and D_2:

$$A_3(t)=\frac{D_2\gamma^2(\nu_2-\nu_3)\left(I_0(\gamma)^2-I_1(\gamma)^2\right)}{-1+\nu_3} \tag{65}$$

$$B_3(t) = 0 \tag{66}$$

$$C_3(t) = C_2 - \frac{D_2\gamma^2(\nu_2 - \nu_3)\left[I_0(\gamma)K_0(\gamma) + I_1(\gamma)K_1(\gamma)\right]}{-1+\nu_3} \tag{67}$$

$$D_3(t) = \frac{D_2(-1+\nu_2)}{-1+\nu_3} \tag{68}$$

Equations (25) and (27) are substituted into equations (32) and (33) in order to find the unknown constants for the coating layer. The matrix system in equation (69) is established to solve for C_2 and D_2:

$$\begin{bmatrix} N1 & N2 \\ N3 & N4 \end{bmatrix}\begin{bmatrix} C_2(t) \\ D_2(t) \end{bmatrix} = \begin{bmatrix} R5 \\ R6 \end{bmatrix} \tag{69}$$

Terms in equation (69) are defined in equations (70) to (75):

$$N1 = -I_0(\gamma) + \frac{I_1(\gamma)}{\gamma} \tag{70}$$

$$N2 = \frac{1}{-1+\nu_3}\left(\begin{array}{l} (-1+\nu_2)\left[(-1+2\nu_3)I_0(\alpha) - \alpha I_1(\alpha)\right] \\ \quad -\gamma^2(\nu_2-\nu_3)\left[I_0(\gamma)^2 - I_1(\gamma)^2\right]\left[\alpha K_0(\alpha) + K_1(\alpha)\right] \\ \quad +\frac{1}{\alpha}\left\{\gamma^2(\nu_2-\nu_3)\left[\alpha I_0(\alpha) - I_1(\alpha)\right]\left[I_0(\gamma)K_0(\gamma) + I_1(\gamma)K_1(\gamma)\right]\right\} \end{array}\right) \tag{71}$$

$$N3 = I_1(\gamma) \tag{72}$$

$$N4 = \frac{1}{-1+\nu_3}\left\{\begin{array}{l} (-1+\nu_2)\left[\alpha I_0(\alpha) - 2(-1+\nu_3)I_1(\alpha)\right] \\ \quad +\gamma^2(\nu_2-\nu_3)\left[-I_0(\gamma)^2 + I_1(\gamma)^2\right]K_1(\alpha) \\ \quad -\gamma^2(\nu_2-\nu_3)I_1(\alpha)\left[I_0(\gamma)K_0(\gamma) + I_1(\gamma)K_1(\gamma)\right] \end{array}\right\} \tag{73}$$

$$R5 = \cos(t\zeta)p(\zeta) \tag{74}$$

$$R6 = \sin(t\zeta)q(\zeta) \tag{75}$$

The solutions of equation (69) for the unknown constants $C_2(t)$ and $D_2(t)$ are shown in equations (76) and (77):

$$C_2(t)=\left(\frac{1}{\Delta_3}\right)\left(\begin{array}{l}-\alpha\left\{\begin{array}{l}(-1+\nu_2)\left[\alpha I_0(\alpha)-2(-1+\nu_3)I_1(\alpha)\right]\\ \quad+\nu^2(\nu_2-\nu_3)\left[-I_0(\gamma)^2+I_1(\gamma)^2\right]K_1(\alpha)\\ \quad-\gamma^2(\nu_2-\nu_3)+I_1(\alpha)\left[I_0(\gamma)K_0(\gamma)+I_1(\gamma)K_1(\gamma)\right]\end{array}\right\}p(\zeta)\cos(t\zeta)\\ +\alpha\left\{\begin{array}{l}(-1+\nu_2)\left[(-1+2\nu_3)I_0(\alpha)-\alpha I_1(\alpha)\right]\\ -\dfrac{-\gamma^2(\nu_2-\nu_3)\left[I_0(\gamma)^2-I_1(\gamma)^2\right]\left[\alpha K_0(\alpha)+K_1(\alpha)\right]}{\alpha}\\ +\dfrac{1}{\alpha}\left\{\gamma^2(\nu_2-\nu_3)\left[\alpha I_0(\alpha)-I_1(\alpha)\right]\left[\begin{array}{l}I_0(\gamma)K_0(\gamma)\\ \quad+I_1(\gamma)K_1(\gamma)\end{array}\right]\right\}\end{array}\right\}q(\zeta)\sin(t\zeta)\end{array}\right) \tag{76}$$

$$D_2(t)=\frac{1}{\Delta_3}\left(\left\{I_1(\alpha)\cos(t\zeta)p(\zeta)-\frac{\left[-\alpha I_0(\alpha)+I_1(\alpha)\right]q(\zeta)\sin(t\zeta)}{\alpha}\right\}\left[-\alpha(-1+\nu_3)\right]\right) \tag{77}$$

Since $A_1(t)$, $B_1(t)$, $A_3(t)$, $B_3(t)$, $C_3(t)$, $D_3(t)$, $C_2(t)$, and $D_2(t)$ are known, the Green's functions in equations (10) to (12)—$F_1(t)$, $F_2(t)$, and $F_3(t)$—are also known.

Displacement Equations

In this investigation, the stability of the interface crack at the matrix-coating interface is examined by calculating the SERR at the leading edge of the crack. The fiber-coating interface is considered to be bonded. Substituting Green's functions for the matrix $F_1(t)$ and coating $F_3(t)$ layers into displacement equations (20) to (23) yields equations (78) to (81). The variables A_1 and B_1 are known from equations (38) and (39); $C_2(t)$ and $D_2(t)$ are known from equations (76) and (77); and $A_3(t)$, $B_3(t)$, $C_3(t)$, and $D_3(t)$ are known from equations (65) to (69).

$$\begin{aligned}u_{r1}(r_1,x) &= -\frac{1}{\pi\mu_1}\int_0^\infty \frac{dF_1}{dr}t\cos(xt)dt\\ &= -\frac{1}{\pi\mu_1}\int_0^\infty t^2\left[-A_1(t)K_1(\rho)-B_1(t)\rho K_0(\rho)\right]\cos(xt)dt\\ &= -\frac{1}{\pi\mu_1}\int_0^\infty t^2\left[\begin{array}{l}-\left(\dfrac{\alpha}{t^3\Delta_1}\left\{\begin{array}{l}p(\xi)\cos(\xi t)\left[\alpha K_0(\alpha)-2(1-\nu_1)K_1(\alpha)\right]\\ \quad+q(\xi)\sin(\xi t)\left[(1-2\nu_1)K_0(\alpha)-\alpha K_1(\alpha)\right]\end{array}\right\}\right)K_1(\rho)\\ \quad-\left(\dfrac{\alpha}{t^3\Delta_1}\left\{\begin{array}{l}-p(\xi)\cos(\xi t)\left[K_1(\alpha)\right]\\ \quad+q(\xi)\sin(\xi t)\left[K_0(\alpha)-\dfrac{K_1(\alpha)}{\alpha}\right]\end{array}\right\}\right)\rho K_0(\rho)\end{array}\right]\cos(xt)dt\end{aligned} \tag{78}$$

$$
\begin{aligned}
&u_{x1}(r_1,x)\\
&=\frac{1}{\pi\mu_1}\int_0^\infty\left[(1-2\nu_1)\nabla^2+\frac{d^2}{dr^2}+\frac{1}{r}\frac{d}{dr}\right]F_1\sin(xt)dt\\
&=\frac{1}{\pi\mu_1}\int_0^\infty t^2\left[2(1-\nu_1)\frac{d^2F_1}{d\rho^2}+2(1-\nu_1)\frac{1}{\rho}\frac{dF_1}{d\rho}+(2\nu_1-1)F_1\right]\sin(xt)dt\\
&=\frac{1}{\pi\mu_1}\int_0^\infty t^2\left\{\begin{array}{l}2(1-\nu_1)\left[A_1(t)K_0(\rho)-B_1(t)K_0(\rho)+\dfrac{A_1(t)}{\rho}K_1(\rho)+B_1(t)\rho K_1(\rho)\right]\\ \quad+2(1-\nu_1)\dfrac{1}{\rho}\left[-A_1(t)K_1(\rho)-B_1(t)\rho K_0(\rho)\right]\\ \quad+(2\nu_1-1)\left[A_1(t)K_0(\rho)+B_1(t)\rho K_1(\rho)\right]\end{array}\right\}\sin(xt)dt\\
&=\frac{1}{\pi\mu_1}\int_0^\infty t^2\left[\begin{array}{l}2(1-\nu_1)\left(\begin{array}{l}\dfrac{\alpha}{t^3\Delta_1}\left\{\begin{array}{l}p(\xi)\cos(\xi t)\left[\alpha K_0(\alpha)-2(1-\nu_1)K_1(\alpha)\right]\\ \quad+q(\xi)\sin(\xi t)\left[(1-2\nu_1)K_0(\alpha)-\alpha K_1(\alpha)\right]\end{array}\right\}\left[K_0(\rho)+\dfrac{K_1(\rho)}{\rho}\right]\\ \quad+\dfrac{\alpha}{t^3\Delta_1}\left\{\begin{array}{l}-p(\xi)\cos(\xi t)\left[K_1(\alpha)\right]\\ \quad+q(\xi)\sin(\xi t)\left[K_0(\alpha)-\dfrac{K_1(\alpha)}{\alpha}\right]\end{array}\right\}\left[K_0(\rho)+\rho K_1(\rho)\right]\end{array}\right)\\ \quad+2(1-\nu_1)\dfrac{1}{\rho}\left(\begin{array}{l}-\dfrac{\alpha}{t^3\Delta_1}\left\{\begin{array}{l}p(\xi)\cos(\xi t)\left[\alpha K_0(\alpha)-2(1-\nu_1)K_1(\alpha)\right]\\ \quad+q(\xi)\sin(\xi t)\left[(1-2\nu_1)K_0(\alpha)-\alpha K_1(\alpha)\right]\end{array}\right\}K_1(\rho)\\ \quad-\dfrac{\alpha}{t^3\Delta_1}\left\{\begin{array}{l}-p(\xi)\cos(\xi t)\left[K_1(\alpha)\right]\\ \quad+q(\xi)\sin(\xi t)\left[K_0(\alpha)-\dfrac{K_1(\alpha)}{\alpha}\right]\end{array}\right\}\rho K_0(\rho)\end{array}\right)\\ \quad+(2\nu_1-1)\left(\begin{array}{l}\dfrac{\alpha}{t^3\Delta_1}\left\{\begin{array}{l}p(\xi)\cos(\xi t)\left[\alpha K_0(\alpha)-2(1-\nu_1)K_1(\alpha)\right]\\ \quad+q(\xi)\sin(\xi t)\left[(1-2\nu_1)K_0(\alpha)-\alpha K_1(\alpha)\right]\end{array}\right\}K_0(\rho)\\ \quad+\dfrac{\alpha}{t^3\Delta_1}\left\{\begin{array}{l}-p(\xi)\cos(\xi t)\left[K_1(\alpha)\right]\\ \quad+q(\xi)\sin(\xi t)\left[K_0(\alpha)-\dfrac{K_1(\alpha)}{\alpha}\right]\end{array}\right\}\rho K_1(\rho)\end{array}\right)\end{array}\right]\sin(xt)dt
\end{aligned}
\tag{79}
$$

$$u_{r3}(r_3,x) = -\frac{1}{\pi\mu_3}\int_0^\infty \frac{dF_3}{dr}\, t\cos(xt)dt$$

$$= -\frac{1}{\pi\mu_3}\int_0^\infty t^2\,\frac{dF_3}{d\rho}\cos(xt)dt$$

$$= -\frac{1}{\pi\mu_3}\int_0^\infty t^2\left[-A_3(t)K_1(\rho) - B_3(t)\rho K_0(\rho) + C_3(t)I_1(\rho) + D_3(t)\rho I_0(\rho)\right]\cos(xt)dt$$

$$= -\frac{1}{\pi\mu_3}\int_0^\infty t^2\left(\begin{array}{l} -\left\{\dfrac{D_2\gamma^2(\nu_2-\nu_3)\left[I_0(\gamma)^2 - I_1(\gamma)^2\right]}{-1+\nu_3}\right\}K_1(\rho) \\ \quad +\left\{C_2 - \dfrac{D_2\gamma^2(\nu_2-\nu_3)\left[I_0(\gamma)K_0(\gamma)+I_1(\gamma)K_1(\gamma)\right]}{-1+\nu_3}\right\}I_1(\rho) \\ \quad +\left[\dfrac{D_2(-1+\nu_2)}{-1+\nu_3}\right]\rho I_0(\rho) \end{array}\right)\cos(xt)dt \tag{80}$$

$$u_{x3}(r_3,x) = \frac{1}{\pi\mu_3}\int_0^\infty\left[(1-2\nu_3)\nabla^2 + \frac{d^2}{dr^2} + \frac{1}{r}\frac{d}{dr}\right]F_3\sin(xt)dt$$

$$= \frac{1}{\pi\mu_3}\int_0^\infty t^2\left[2(1-\nu_3)\frac{d^2F_3}{d\rho^2} + 2(1-\nu_3)\frac{1}{\rho}\frac{dF_3}{d\rho} + (2\nu_3-1)F_3\right]\sin(xt)dt$$

$$= \frac{1}{\pi\mu_3}\int_0^\infty t^2\left\{\begin{array}{l} A_3(t)K_0(\rho) + B_3(t)\left[\rho K_1(\rho) - 4(1-\nu_3)K_0(\rho)\right] \\ \quad + C_3(t)I_0(\rho) + D_3(t)\left[\rho I_1(\rho) + 4(1-\nu_3)I_0(\rho)\right] \end{array}\right\}\sin(xt)dt$$

$$= \frac{1}{\pi\mu_3}\int_0^\infty t^2\left(\begin{array}{l} \left\{\dfrac{D_2\gamma^2(\nu_2-\nu_3)\left[I_0(\gamma)^2 - I_1(\gamma)^2\right]}{-1+\nu_3}\right\}K_0(\rho) \\ \quad +\left\{C_2 - \dfrac{D_2\gamma^2(\nu_2-\nu_3)\left[I_0(\gamma)K_0(\gamma)+I_1(\gamma)K_1(\gamma)\right]}{-1+\nu_3}\right\}I_0(\rho) \\ \quad +\left[\dfrac{D_2(-1+\nu_2)}{-1+\nu_3}\right]\left[\rho I_1(\rho) + 4(1-\nu_3)I_0(\rho)\right] \end{array}\right)\sin(xt)dt \tag{81}$$

Using the same methods, a solution with a similar form can be obtained for antisymmetric loading conditions. The solutions for symmetric and antisymmetric loading conditions can be rewritten as equations (82) to (85), where $J_{11}^{1}(t,r)$, $J_{12}^{1}(t,r)$, $J_{21}^{1}(t,r)$, $J_{22}^{1}(t,r)$, $J_{11}^{3}(t,r)$, $J_{12}^{3}(t,r)$, $J_{21}^{3}(t,r)$, $J_{22}^{3}(t,r)$, Δ_1, and Δ_3 are defined in equations (86) to (95):

$$u_{r1}(r,x)=\frac{1}{\pi\mu_1}\left[-p(\xi)\int_0^\infty J_{11}^{1}(t,r)\begin{pmatrix}\cos(t\xi)\cos(xt)\\ \sin(t\xi)\sin(xt)\end{pmatrix}\frac{dt}{t}+q(\xi)\int_0^\infty J_{12}^{1}(t,r)\begin{pmatrix}\sin(t\xi)\cos(xt)\\ -\cos(t\xi)\sin(xt)\end{pmatrix}\frac{dt}{t}\right] \quad (82)$$

$$u_{r3}(r,x)=-\frac{1}{\pi\mu_3}\left[p(\xi)\int_0^\infty J_{11}^{3}(t,r)\begin{pmatrix}\cos(t\xi)\cos(xt)\\ \sin(t\xi)\sin(xt)\end{pmatrix}\frac{dt}{t}+q(\xi)\int_0^\infty J_{12}^{3}(t,r)\begin{pmatrix}\sin(t\xi)\cos(xt)\\ -\cos(t\xi)\sin(xt)\end{pmatrix}\frac{dt}{t}\right] \quad (83)$$

$$u_{x1}(r,x)=\frac{1}{\pi\mu_1}\left[p(\xi)\int_0^\infty J_{21}^{1}(t,r)\begin{pmatrix}\cos(t\xi)\sin(xt)\\ -\sin(t\xi)\cos(xt)\end{pmatrix}\frac{dt}{t}+q(\xi)\int_0^\infty J_{22}^{1}(t,r)\begin{pmatrix}\sin(t\xi)\sin(xt)\\ \cos(t\xi)\cos(xt)\end{pmatrix}\frac{dt}{t}\right] \quad (84)$$

$$u_{x3}(r,x)=\frac{1}{\pi\mu_3}\left[p(\xi)\int_0^\infty J_{21}^{3}(t,r)\begin{pmatrix}\cos(t\xi)\sin(xt)\\ -\sin(t\xi)\cos(xt)\end{pmatrix}\frac{dt}{t}+q(\xi)\int_0^\infty J_{22}^{3}(t,r)\begin{pmatrix}\sin(t\xi)\sin(xt)\\ \cos(t\xi)\cos(xt)\end{pmatrix}\frac{dt}{t}\right] \quad (85)$$

where

$$J_{11}^{1}(t,r)=\frac{1}{\Delta_1}\left\{\left[-\alpha^2K_0(\alpha)+2(1-\nu_1)\alpha K_1(\alpha)\right]K_1(\rho)+\left[\alpha K_1(\alpha)\right]\rho K_0(\rho)\right\} \quad (86)$$

$$J_{12}^{1}(t,r)=\frac{1}{\Delta_1}\left\{\left[(1-2\nu_1)\alpha K_0(\alpha)-\alpha^2K_1(\alpha)\right]K_1(\rho)+\left[\alpha K_0(\alpha)+K_1(\alpha)\right]\rho K_0(\rho)\right\} \quad (87)$$

$$J_{21}^{1}(t,r)=\frac{1}{\Delta_1}\left\{\left[\alpha^2K_0(\alpha)-2\alpha(1-\nu_1)K_1(\alpha)\right]K_0(\rho)-\alpha K_1(\alpha)\left[\rho K_1(\rho)-4(1-\nu_1)K_0(\rho)\right]\right\} \quad (88)$$

$$J_{22}^{1}(t,r)=\frac{1}{\Delta_1}\left\{\left[(1-2\nu_1)\alpha K_0(\alpha)-\alpha^2K_1(\alpha)\right]K_0(\rho)-\left[\alpha K_0(\alpha)+K_1(\alpha)\right]\left[\rho K_1(\rho)-4(1-\nu_1)K_0(\rho)\right]\right\} \quad (89)$$

$$J_{11}^{3}(r,t)=\frac{\alpha}{\Delta 3}\left\{\begin{array}{l}(-1+\nu_2)\rho I_0(\rho)I_1(\alpha)+I_1(\rho)(1-\nu_2)\left[\begin{array}{l}\alpha I_0(\alpha)-2(-1+\nu_3)I_1(\alpha)\\ \quad+\gamma^2(\nu_2-\nu_3)I_0(\gamma)^2-I_1(\gamma)^2)K_1(\alpha)\end{array}\right]\\ \quad+\gamma^2(\nu_2-\nu_3)I_1(\alpha)\left[-I_0(\gamma)^2+I_1(\gamma)^2\right]K_1(\rho)\end{array}\right\} \quad (90)$$

$$J_{12}^{3}(r,t)=\frac{1}{\Delta_3}\left\{\alpha\left[\begin{array}{l}\dfrac{(-1+\nu_2)\rho I_0(\rho)\left[\alpha I_0(\alpha)-I_1(\alpha)\right]}{\alpha}\\ \quad -\dfrac{1}{\alpha}\left(I_1(\rho)\left\{\begin{array}{l}-\alpha(-1+\nu_2)(-1+2\nu_3)I_0(\alpha)+\alpha^2(-1+\nu_2)I_1(\alpha)\\ \quad +\gamma^2(\nu_2-\nu_3)\left[I_0(\gamma)^2-I_1(\gamma)^2\right]\left[\alpha K_0(\alpha)+K_1(\alpha)\right]\end{array}\right\}\right)\\ \quad +\gamma^2(\nu_2-\nu_3)\left[-I_0(\alpha)+\dfrac{I_1(\alpha)}{\alpha}\right]\left[I_0(\gamma)^2-I_1(\gamma)^2\right]K_1(\rho)\end{array}\right]\right\} \tag{91}$$

$$J_{21}^{3}=\frac{1}{\Delta_3}\left(\begin{array}{l}\alpha(-1+\nu_2)I_1(\alpha)\left[-4(-1+\nu_3)I_0(\rho)+\rho I_1(\rho)\right]+\alpha\nu^2(\nu_2-\nu_3)I_1(\alpha)\left[I_0(\gamma)^2-I_1(\gamma)^2\right]K_0(\rho)\\ \quad -\alpha I_0(\rho)\left\{(-1+\nu_2)\left[\alpha I_0(\alpha)-2(-1+\nu_3)I_1(\alpha)\right]+\gamma^2(\nu_2-\nu_3)\left[-I_0(\gamma)^2+I_1(\gamma^2)\right]K_1(\alpha)\right\}\end{array}\right) \tag{92}$$

$$J_{22}^{3}=\frac{1}{\Delta_3}\left[\begin{array}{l}(1-\nu_2)\left[\alpha I_0(\alpha)-I_1(\alpha)\right]\left[4(-1+\nu_3)I_0(\rho)-\rho I_1(\rho)\right]+\gamma^2(\nu_2-\nu_3)\\ \quad \left(\begin{array}{l}\alpha I_0(\alpha)-I_1(\alpha)\left[I_0(\gamma)^2-I_1(\gamma)^2\right]K_0(\rho)\\ \quad -I_0(\rho)\left\{\begin{array}{l}-\alpha(-1+\nu_2)(-1+2\nu_3)I_0(\alpha)+\alpha^2(-1+\nu_2)I_1(\alpha)\\ \quad +\gamma^2(\nu_2-\nu_3)\left[I_0(\gamma)^2-I_1(\gamma)^2\right]\left[\alpha K_0(\alpha)+K_1(\alpha)\right]\end{array}\right\}\end{array}\right)\end{array}\right] \tag{93}$$

$$\Delta_1=-\alpha^2 K_0{}^2(\alpha)+\left[\alpha^2+2(1-\nu_1)\right]K_1{}^2(\alpha) \tag{94}$$

$$\Delta_3=\left[\begin{array}{l}\alpha^2(-1+\nu_2)I_0(\alpha)^2-\gamma^2(\nu_2-\nu_3)I_0(\gamma)^2\\ \quad -(-1+\nu_2)\left(2+\alpha^2-2\nu_3\right)I_1(\alpha)^2+\gamma^2(\nu_2-\nu_3)I_1(\gamma)^2\end{array}\right] \tag{95}$$

Integral Equations

The stress-related boundary conditions at the matrix-coating interface are given by equations (96) and (97):

$$\sigma_{r1}(r_c,x)=\sigma_{r3}(r_c,x)=p(x)\qquad x\in(L+L') \tag{96}$$

$$\tau_{rx1}(r_c,x)=\tau_{rx3}(r_c,x)=q(x)\qquad x\in(L+L') \tag{97}$$

where L is the length of the bonded surface and L' is the length of the crack surface. The functions $p(x)$ and $q(x)$ are zero on the crack surface and unknown on the bonded surface. The displacement-related boundary conditions at the matrix-coating (region 1 to region 3) interface are given by equations (98) and (99):

$$u_{r1}(r_c,x)-u_{r3}(r_c,x)=g_1(x)\qquad x\in L \tag{98}$$

$$u_{x1}(r_c,x)-u_{x3}(r_c,x)=g_2(x) \qquad x\in L \tag{99}$$

For the symmetric case,

$$\begin{aligned} p(x)&=p(-x)\\ q(x)&=-q(-x)\\ g_1(x)&=g_1(-x)\\ g_2(x)&=-g_2(-x) \end{aligned} \tag{100}$$

For the antisymmetric case,

$$\begin{aligned} p(x)&=-p(-x)\\ q(x)&=q(-x)\\ g_1(x)&=-g_1(-x)\\ g_2(x)&=g_2(-x) \end{aligned} \tag{101}$$

The problem is solved if $p(x)$ and $q(x)$ on L are determined. In order to find these functions along the bonded surface L, the integral equations are obtained by substituting equations (81) to (84) into equations (99) to (100). For the symmetric loading condition, the integral equations (99) and (100) become equations (102) and (103):

$$\lim_{r\to a}\left[\frac{1}{\pi}\left(\begin{aligned}&\int_0^\infty\left\{\int_0^\infty\left[-\frac{J_{11}^1(t,r)}{\mu_1}+\frac{J_{11}^3(t,r)}{\mu_3}\right]\left[\cos(t\xi)\cos(xt)\right]\frac{dt}{t}\right\}p(\xi)d\xi\\ &\quad+\int_0^\infty\left\{\int_0^\infty\left[\frac{J_{12}^1(t,r)}{\mu_1}+\frac{J_{12}^3(t,r)}{\mu_3}\right]\left[\sin(t\xi)\cos(xt)\right]\frac{dt}{t}\right\}q(\xi)d\xi\end{aligned}\right)\right]=g_1(x) \tag{102}$$

$$\lim_{r\to a}\left[-\frac{1}{\pi}\left(\begin{aligned}&\int_0^\infty\left\{\int_0^\infty\left[\frac{J_{21}^1(t,r)}{\mu_1}-\frac{J_{21}^3(t,r)}{\mu_3}\right]\left[\cos(t\xi)\sin(xt)\right]\frac{dt}{t}\right\}p(\xi)d\xi\\ &\quad+\int_0^\infty\left\{\int_0^\infty\left[-\frac{J_{22}^1(t,r)}{\mu_1}-\frac{J_{22}^3(t,r)}{\mu_3}\right]\left[\sin(t\xi)\sin(xt)\right]\frac{dt}{t}\right\}q(\xi)d\xi\end{aligned}\right)\right]=g_2(x) \tag{103}$$

For the antisymmetric loading condition, the integral equations (99) and (100) become equations (104) and (105):

$$\lim_{r\to a}\left[\frac{1}{\pi}\left(\begin{aligned}&\int_0^\infty\left\{\int_0^\infty\left[-\frac{J_{11}^1(t,r)}{\mu_1}+\frac{J_{11}^3(t,r)}{\mu_3}\right]\left[\sin(t\xi)\sin(xt)\right]\frac{dt}{t}\right\}p(\xi)d\xi\\ &\quad+\int_0^\infty\left\{\int_0^\infty\left[\frac{J_{12}^1(t,r)}{\mu_1}+\frac{J_{12}^3(t,r)}{\mu_3}\right]\left[-\cos(t\xi)\sin(xt)\right]\frac{dt}{t}\right\}q(\xi)d\xi\end{aligned}\right)\right]=g_1(x) \tag{104}$$

$$\lim_{r\to a}\left[\frac{1}{\pi}\left(\begin{array}{l}\displaystyle\int_0^\infty\left\{\int_0^\infty\left[\frac{J_{21}^1(t,r)}{\mu_1}-\frac{J_{21}^3(t,r)}{\mu_3}\right]\left[-\sin(t\xi)\cos(xt)\right]\frac{dt}{t}\right\}p(\xi)d\xi \\ \quad\displaystyle+\int_0^\infty\left\{\int_0^\infty\left[-\frac{J_{22}^1(t,r)}{\mu_1}-\frac{J_{22}^3(t,r)}{\mu_3}\right]\left[\cos(t\xi)\cos(xt)\right]\frac{dt}{t}\right\}q(\xi)d\xi\end{array}\right)\right]=g_2(x) \tag{105}$$

For the combined symmetric and antisymmetric loading condition, the integral equations are given by equations (106) and (107):

$$\lim_{r\to a}\left[\frac{1}{2\pi}\left(\begin{array}{l}\displaystyle\int_0^\infty\left\{\int_0^\infty\left[-\frac{J_{11}^1(t,r)}{\mu_1}+\frac{J_{11}^3(t,r)}{\mu_3}\right]\left[\begin{array}{l}\cos(t\xi)\cos(xt)\\ \quad+\sin(t\xi)\sin(xt)\end{array}\right]\frac{dt}{t}\right\}p(\xi)d\xi \\ \quad\displaystyle+\int_0^\infty\left\{\int_0^\infty\left[\frac{J_{12}^1(t,r)}{\mu_1}+\frac{J_{12}^3(t,r)}{\mu_3}\right]\left[\begin{array}{l}\sin(t\xi)\cos(xt)\\ \quad-\cos(t\xi)\sin(xt)\end{array}\right]\frac{dt}{t}\right\}q(\xi)d\xi\end{array}\right)\right]=g_1(x) \tag{106}$$

$$\lim_{r\to a}\left[\frac{1}{2\pi}\left(\begin{array}{l}\displaystyle\int_0^\infty\left\{\int_0^\infty\left[\frac{J_{21}^1(t,r)}{\mu_1}-\frac{J_{21}^3(t,r)}{\mu_3}\right]\left[\begin{array}{l}\cos(t\xi)\sin(xt)\\ \quad-\sin(t\xi)\cos(xt)\end{array}\right]\frac{dt}{t}\right\}p(\xi)d\xi \\ \quad\displaystyle+\int_0^\infty\left\{\int_0^\infty\left[-\frac{J_{22}^1(t,r)}{\mu_1}-\frac{J_{22}^3(t,r)}{\mu_3}\right]\left[\begin{array}{l}\sin(t\xi)\sin(xt)\\ \quad+\cos(t\xi)\cos(xt)\end{array}\right]\frac{dt}{t}\right\}q(\xi)d\xi\end{array}\right)\right]=g_2(x) \tag{107}$$

The upper and lower kernels correspond to symmetric and antisymmetric cases, respectively. Considering the symmetry properties of the functions $p(x)$, $q(x)$, $g_1(x)$, and $g_2(x)$—which are given by equations (100) and (101)—and using trigonometric identities enables the integral to be rewritten as equations (108) and (109):

$$\lim_{r\to a}\left[\frac{1}{2\pi}\left(\begin{array}{l}\displaystyle\int_0^\infty\left\{\int_0^\infty\left[-\frac{J_{11}^1(t,r)}{\mu_1}+\frac{J_{11}^3(t,r)}{\mu_3}\right]\cos(\xi-x)\frac{dt}{t}\right\}p(\xi)d\xi \\ \quad\displaystyle+\int_0^\infty\left\{\int_0^\infty\left[\frac{J_{12}^1(t,r)}{\mu_1}+\frac{J_{12}^3(t,r)}{\mu_3}\right]\sin(\xi-x)\frac{dt}{t}\right\}q(\xi)d\xi\end{array}\right)\right]=g_1(x) \tag{108}$$

$$\lim_{r\to a}\left[\frac{1}{2\pi}\left(\begin{array}{l}\displaystyle\int_0^\infty\left\{\int_0^\infty\left[\frac{J_{21}^1(t,r)}{\mu_1}-\frac{J_{21}^3(t,r)}{\mu_3}\right]\left[\sin(\xi-x)\right]\frac{dt}{t}\right\}p(\xi)d\xi \\ \quad\displaystyle+\int_0^\infty\left\{\int_0^\infty\left[-\frac{J_{22}^1(t,r)}{\mu_1}-\frac{J_{22}^3(t,r)}{\mu_3}\right]\left[\cos(\xi-x)\right]\frac{dt}{t}\right\}q(\xi)d\xi\end{array}\right)\right]=g_2(x) \tag{109}$$

Equations (108) and (109) become equations (110) and (111) with the terms defined in equation (112):

$$\lim_{r\to a}\left(\frac{1}{2\pi}\left\{\begin{array}{l}\int_0^\infty\left[\int_0^\infty H_{11}(t,r)\cos(\xi-x)t\,\frac{dt}{t}\right]p(\xi)d\xi \\ \quad+\int_0^\infty\left[\int_0^\infty H_{12}(t,r)\sin(\xi-x)t\,\frac{dt}{t}\right]q(\xi)d\xi\end{array}\right\}\right)=g_1(x) \tag{110}$$

and

$$\lim_{r\to a}\left[\frac{1}{2\pi}\left(\begin{array}{l}-\int_0^\infty\left\{\int_0^\infty H_{21}(t,r)\left[\sin(\xi-x)\right]\frac{dt}{t}\right\}p(\xi)d\xi \\ \quad+\int_0^\infty\left\{\int_0^\infty H_{22}(t,r)\left[\cos(\xi-x)\right]\frac{dt}{t}\right\}q(\xi)d\xi\end{array}\right)\right]=g_2(x) \tag{111}$$

where

$$\begin{aligned}H_{11}(t,r)&=-\frac{J_{11}^1(t,r)}{\mu_1}+\frac{J_{11}^3(t,r)}{\mu_3}\\ H_{12}(t,r)&=\frac{J_{12}^1(t,r)}{\mu_1}+\frac{J_{12}^3(t,r)}{\mu_3}\\ H_{21}(t,r)&=\frac{J_{21}^1(t,r)}{\mu_1}+\frac{J_{21}^3(t,r)}{\mu_3}\\ H_{22}(t,r)&=-\frac{J_{22}^1(t,r)}{\mu_1}-\frac{J_{22}^3(t,r)}{\mu_3}\end{aligned} \tag{112}$$

Since the inner integral for t cannot be integrated using usual integration methods, an asymptotic approach is applied. When the asymptotic expansions of $H_{ij}(t, r)$ are considered as $t \to 0$, some of the kernels will diverge. For divergent kernels to be avoided, the $1/t$ factor must be removed. For this reason, equations (110) and (111) are differentiated with respect to x. Using the identities in equations (113) and (114) changes equations (111) and (112) into equations (115) and (116):

$$\frac{d}{dx}\cos(\alpha-x)t=t\sin(\alpha-x)t \tag{113}$$

$$\frac{d}{dx}\sin(\alpha-x)t=-t\cos(\alpha-x)t \tag{114}$$

$$\lim_{r\to a}\left(\frac{1}{2\pi}\left\{\begin{array}{l}\int_0^\infty\left[\int_0^\infty H_{11}(t,r)\sin(\xi-x)dt\right]p(\xi)d\xi \\ \quad-\int_0^\infty\left[\int_0^\infty H_{12}(t,r)\cos(\xi-x)dt\right]q(\xi)d\xi\end{array}\right\}\right)=g_1'(x) \tag{115}$$

$$\lim_{r\to a}\left[\frac{1}{2\pi}\left(\begin{array}{l}\int_0^\infty\left\{\int_0^\infty H_{21}(t,r)\left[\cos(\xi-x)\right]dt\right\}p(\xi)d\xi \\ \qquad +\int_0^\infty\left\{\int_0^\infty H_{22}(t,r)\left[\sin(\xi-x)\right]dt\right\}q(\xi)d\xi\end{array}\right)\right]=g_2'(x) \tag{116}$$

Integration of equations (115) and (116) using an asymptotic approach gives equations (117) and (118) and the terms in equation (119):

$$\lim_{r\to a}\left\{\frac{1}{2\pi}\left[\int_0^\infty W_1 p(\xi)d\xi-\int_0^\infty W_2 q(\xi)d\xi\right]\right\}=g_1'(x) \tag{117}$$

$$\lim_{r\to a}\left\{\frac{1}{2\pi}\left[\int_0^\infty W_3 p(\xi)d\xi+\int_0^\infty W_4 q(\xi)d\xi\right]\right\}=g_2'(x) \tag{118}$$

where

$$\begin{aligned}
W_1&=\int_0^\infty\left[H_{11}(t,r)-H_{11}^\infty(t,r)\right]\sin(\xi-x)dt+\int_0^\infty H_{11}^\infty(t,r)\sin(\xi-x)dt\\
W_2&=\int_0^\infty\left[H_{12}(t,r)-H_{12}^\infty(t,r)\right]\cos(\xi-x)dt+\int_0^\infty H_{12}^\infty(t,r)\cos(\xi-x)dt\\
W_3&=\int_0^\infty\left[H_{21}(t,r)-H_{21}^\infty(t,r)\right]\cos(\xi-x)dt+\int_0^\infty H_{21}^\infty(t,r)\cos(\xi-x)dt\\
W_4&=\int_0^\infty\left[H_{22}(t,r)-H_{22}^\infty(t,r)\right]\sin(\xi-x)dt+\int_0^\infty H_{22}^\infty(t,r)\sin(\xi-x)dt
\end{aligned} \tag{119}$$

Singular Integral Equations and Fredholm Kernels

In the problem considered here, the bonding stresses p and q are unknown, and g_1 and g_2 are the known displacement differences. Therefore, the displacement-related equations (98) and (99) are used to find p and q. From these two boundary conditions, two integral equations are constructed to find the two unknowns. In equations (117) and (118), sine and cosine terms are the steady-state oscillating functions. Therefore, $H_{ij}(t, r)$ determines the behavior of the integrals for these equations. For the integrals in equations (117) and (118) to be calculated for a given interval, the integrand must be integrable over the corresponding domain. If the constant terms at infinity in $H_{ij}(t, r)$ are subtracted from $H_{ij}(t, r)$, the functions $H_{ij}(t, r) - H^{\infty}_{ij}(t, r)$ become integrable. After the asymptotic values are subtracted and added, the integral equations become SIEs with two parts. The dominant parts contain the singularities, and the regular parts are the Fredholm kernels. After the asymptotic part is subtracted, the kernels can be integrated numerically. But this subtracted quantity has to be added back to the whole equation. That is where the dominant part of the SIE comes from. If the limit is taken as $\varepsilon \to 0$ and $r \to r_c$ in the integral equations, the Fredholm kernels and the SIEs in equations (117) and (118) become equations (120) and (121):

$$\begin{aligned}
\frac{\mu_0}{2\mu_1\mu_3(1-\nu_3)}&\left\{-\gamma^* q(x)-\frac{1}{\pi}\int_a^b\frac{p(t)}{t-x}dt-\frac{1}{\pi}\int_a^b\left[k_{11}(x,t)p(t)+k_{12}(x,t)q(t)\right]dt\right\}=g_1'(x)\\
&-\gamma^* q(x)-\frac{1}{\pi}\int_a^b\frac{p(t)}{t-x}dt-\frac{1}{\pi}\int_a^b\left[k_{11}(x,t)p(t)+k_{12}(x,t)q(t)\right]dt=Q_1(x)
\end{aligned} \tag{120}$$

$$\frac{\mu_0}{2\mu_1\mu_3(1-\nu_3)}\left\{\gamma^* p(x)-\frac{1}{\pi}\int_a^b \frac{q(t)}{t-x}dt+\frac{1}{\pi}\int_a^b\left[k_{21}(x,t)p(t)+k_{22}(x,t)q(t)\right]dt\right\}=g_2'(x)$$

$$\gamma^* p(x)-\frac{1}{\pi}\int_a^b \frac{q(t)}{t-x}dt+\frac{1}{\pi}\int_a^b\left[k_{21}(x,t)p(t)+k_{22}(x,t)q(t)\right]dt=Q_2(x) \tag{121}$$

where $a \le x \le b$ and $a \le t \le b$.

$$\gamma^* = \frac{1}{\mu_0}\left\{\left[(1-2\nu_1)(1-\nu_3)\right]\mu_3-\left[(1-2\nu_2)(1-\nu_3)\right]\mu_1\right\} \tag{122}$$

$$\mu_0 = 2\mu_3(1-\nu_1)(1-\nu_3)+2\mu_1(1-\nu_2)(1-\nu_3) \tag{123}$$

$$k_{11}(x,t)=\int_0^\infty\left(\begin{array}{l}\dfrac{(1-\nu_3)\mu_3}{\mu_0}\left(\dfrac{\left\{2(1-\nu_1)\alpha\left[K_1(\alpha)\right]^2\right\}}{\Delta_1}-2(1-\nu_1)\right)\\ \quad+\dfrac{\mu_1}{\mu_0}\left\{\dfrac{2\alpha(-1+\nu_2)(1-\nu_3)^2\left[I_1(\alpha)\right]^2}{\Delta_3}-2(1-\nu_2)(1-\nu_3)\right\}\end{array}\right)\sin\left[(t-x)s\right]dt \tag{124}$$

$$k_{12}(x,t)=k_{21}(x,t)=$$

$$\int_0^\infty\left\{\begin{array}{l}\dfrac{(1-\nu_3)\mu_3}{\mu_0}\left[\dfrac{1}{\Delta_1}\left(\begin{array}{l}\left\{\alpha^2\left[K_0(\alpha)\right]^2+2(1-\nu_1)\alpha K_0(\alpha)K_1(\alpha)\right\}\\ \quad-\alpha^2\left[K_1(\alpha)\right]^2\end{array}\right)-(1-2\nu_1)\right]\\ \quad-\dfrac{\mu_1}{\mu_0}\left(\dfrac{(1-\nu_3)}{\Delta_3}\left\{\begin{array}{l}\alpha^2(-1+\nu_2)\left[I_1(\alpha)\right]^2\\ \quad-\gamma^2(\nu_2-\nu_3)\left[I_0(\gamma)\right]^2\\ \quad+2\alpha(-1+\nu_2)(1-\nu_3)I_0(\alpha)I_1(\alpha)\\ \quad-\alpha^2(-1+\nu_2)\left[I_0(\alpha)\right]^2\\ \quad+\gamma^2(\nu_2-\nu_3)\left[I_1(\gamma)\right]^2\end{array}\right)-(1-2\nu_2)(1-\nu_3)\right)\end{array}\right\}\cos\left[(t-x)s\right]ds \tag{125}$$

$$k_{22}(x,t)=\int_0^\infty \left[\begin{array}{l} \dfrac{(1-\nu_3)\mu_3}{\mu_0}\left\{ \dfrac{1}{\Delta_1}\left[\begin{array}{l} (3-2\nu_1)\alpha K_0^2(\alpha) \\ \quad +4(1-\nu_1)K_0(\alpha)K_1(\alpha) \\ \quad -\alpha K_1^2(\alpha) \end{array} \right](-2(1-\nu_1)) \right\} \\ \quad +\dfrac{\mu_1}{\mu_0}\left(\dfrac{(1-\nu_3)}{\Delta_3}\left\{ \begin{array}{l} \alpha(-1+\nu_2)(3-2\nu_3)I_0^2(\alpha) \\ \quad -4(-1+\nu_2)(1-\nu_3)I_0(\alpha)I_1(\alpha) \\ \quad -\gamma^2(\nu_2-\nu_3)\left[I_0^2(\gamma)-I_1^2(\gamma)\right]K_0(\alpha) \\ \quad -\gamma^2(\nu_2-\nu_3)\left[I_0^2(\gamma)-I_1^2(\gamma)\right]K_1(\alpha) \\ \quad +\alpha(-1+\nu_2)I_1^2(\alpha) \end{array} \right) \right. \\ \left. \quad -2(1-\nu_2)(1-\nu_3) \right) \end{array} \right] \sin\left[(t-x)s\right]ds \tag{126}$$

$$\alpha = r_c t,\ \ \gamma = r_f t$$

$$\Delta_1 = -\alpha^2 K_0^2(\alpha)+\left[\alpha^2+2(1-\nu_1)\right]K_1^2(\alpha) \tag{127}$$

$$\Delta_3 = \left[\begin{array}{l} \alpha^2(-1+\nu_2)I_0(\alpha)^2-\gamma^2(\nu_2-\nu_3)I_0(\gamma)^2 \\ \quad -(-1+\nu_2)\left(2+\alpha^2-2\nu_3\right)I_1(\alpha)^2+\gamma^2(\nu_2-\nu_3)I_1(\gamma)^2 \end{array} \right] \tag{128}$$

$$Q_1 = 2(1-\nu_3)\frac{\mu_1\mu_3}{\mu_0}g_1'(x)$$

$$Q_2 = 2(1-\nu_3)\frac{\mu_1\mu_3}{\mu_0}g_2'(x) \tag{129}$$

Verification of the Singular Integral Equation

For verification of the analytical result, the SIEs for the three-concentric-cylinder model can be easily reduced to the model with two concentric cylinders developed by Ozbek and Erdogan (ref. 5). Making the material properties of the coating equal to the material properties of the fiber (i.e., $\mu_3 = \mu_2$, $\nu_3 = \nu_2$, and $E_2 = E_3$) in equations (120) and (121) yields exactly the same SIEs as in equation 14 of reference 5, as shown in equations (130) and (131):

$$-\tilde{\gamma}_2^{\,*}q(x)-\frac{1}{\pi}\int_a^b\frac{p(t)}{t-x}dt-\frac{1}{\pi}\int_a^b\left[\tilde{k}_{11}(x,t)p(t)+\tilde{k}_{12}(x,t)q(t)\right]dt=\tilde{Q}_1(x) \tag{130}$$

$$\tilde{\gamma}_2^{\,*}p(x)-\frac{1}{\pi}\int_a^b\frac{q(t)}{t-x}dt+\frac{1}{\pi}\int_a^b\left[\tilde{k}_{21}(x,t)p(t)+\tilde{k}_{22}(x,t)q(t)\right]dt=\tilde{Q}_2(x) \tag{131}$$

where the kernels γ_2^* are reduced to the one in reference 5 as shown in the following equation:

$$a \le x \le b \quad a \le t \le b$$

$$\mu_0 = 2\mu_2(1-\nu_1)(1-\nu_2) + 2\mu_1(1-\nu_2)(1-\nu_2)$$

$$\mu_0 = (1-\nu_2)\tilde{\mu}_0 \tag{132}$$

$$\gamma_2^* = \frac{(1-\nu_2)}{\mu_0}\left[(1-2\nu_1)\mu_2 - (1-2\nu_2)\mu_1\right]$$

$$\gamma_2^* = \frac{1}{\tilde{\mu}_0}\left[(1-2\nu_1)\mu_2 - (1-2\nu_2)\mu_1\right]$$

$$\gamma_2^* = \tilde{\gamma}_2^* \tag{133}$$

$$k_{11}(x,t) = \int_0^\infty \left(\begin{array}{l} \dfrac{(1-\nu_2)\mu_2}{(1-\nu_2)\tilde{\mu}_0}\left(\dfrac{\left\{2(1-\nu_1)\alpha\left[K_1(\alpha)\right]^2\right\}}{\tilde{\Delta}_1} - 2(1-\nu_1) \right) \\ \quad + \dfrac{(1-\nu_2)\mu_1}{(1-\nu_2)\tilde{\mu}_0}\left\{ \dfrac{2\alpha(-1+\nu_2)(1-\nu_2)\left[I_1(\alpha)\right]^2}{(-1+\nu_2)\tilde{\Delta}_2} - 2(1-\nu_2) \right\} \end{array} \right) \sin\left[(t-x)s\right]dt$$

$$k_{11}(x,t) = \tilde{k}_{11}(x,t) \tag{134}$$

$$k_{12}(x,t) = k_{21}(x,t)$$

$$= \int_0^\infty \left\{ \begin{array}{l} \dfrac{(1-\nu_2)\mu_2}{(1-\nu_2)\tilde{\mu}_0}\left[\dfrac{1}{\tilde{\Delta}_1}\left(\left\{ \begin{array}{l} \alpha^2\left[K_0(\alpha)\right]^2 \\ \quad + 2(1-\nu_1)\alpha K_0(\alpha)K_1(\alpha) \end{array} \right\} - \alpha^2\left[K_1(\alpha)\right]^2 \right) \right] \\ \quad - (1-2\nu_1) \\ -\dfrac{(1-\nu_2)\mu_1}{(1-\nu_2)\tilde{\mu}_0}\left(\dfrac{1}{(-1+\nu_2)\tilde{\Delta}_2}\left\{ \begin{array}{l} \alpha^2(-1+\nu_2)\left[I_1(\alpha)\right]^2 \\ \quad + 2\alpha(-1+\nu_2)(1-\nu_2)I_0(\alpha)I_1(\alpha) \\ \quad - \alpha^2(-1+\nu_2)\left[I_0(\alpha)\right]^2 \end{array} \right\} \right. \\ \left. \quad - (1-2\nu_2) \right) \end{array} \right\} \cos\left[(t-x)s\right]ds$$

$$k_{12}(x,t) = k_{21}(x,t) = \tilde{k}_{12}(x,t) = \tilde{k}_{21}(x,t) \tag{135}$$

$$k_{22}(x,t)$$

$$= \int_0^\infty \left[\begin{array}{l} \dfrac{(1-\nu_2)\mu_2}{(1-\nu_2)\tilde{\mu}_0} \left\{ \dfrac{1}{\tilde{\Delta}_1} \left[\begin{array}{l} (3-2\nu_1)\alpha K_0^2(\alpha) \\ \quad +4(1-\nu_1)K_0(\alpha)K_1(\alpha) - \alpha K_1^2(\alpha) \end{array} \right] - 2(1-\nu_1) \right\} \\ \quad + \dfrac{(1-\nu_2)\mu_1}{(1-\nu_2)\tilde{\mu}_0} \left(\begin{array}{l} \dfrac{1}{(-1+\nu_2)\tilde{\Delta}_2} \left\{ \begin{array}{l} \alpha(-1+\nu_2)(3-2\nu_2)I_0^2(\alpha) \\ \quad -4(-1+\nu_2)(1-\nu_2)I_0(\alpha)I_1(\alpha) \\ \quad -\dfrac{1}{\alpha}\left[\alpha^2(-1+\nu_2)I_1^2(\alpha)\right] \end{array} \right. \\ \quad -2(1-\nu_2) \end{array} \right) \end{array} \right] \sin\left[(t-x)s\right] ds$$

$$k_{22}(x,t) = \tilde{k}_{22}(x,t) \tag{136}$$

$$\alpha = r_f t \quad \gamma = r_f t$$

$$\Delta_1 = -\alpha^2 K_0{}^2(\alpha) + \left[\alpha^2 + 2(1-\nu_1)\right] K_1{}^2(\alpha)$$

$$\Delta_1 = \tilde{\Delta}_1 \tag{137}$$

$$\Delta_2 = \alpha^2(-1+\nu_2)I_0(\alpha)^2 - (-1+\nu_2)(2+\alpha^2-2\nu_2)I_1(\alpha)^2$$

$$\Delta_2 = (-1+\nu_2)\tilde{\Delta}_2 \tag{138}$$

Therefore, the validity of the left side of the SIEs (eqs. (120) and (121)) are established. Reducing the right side of the SIEs (eqs. (120) and (121)) to the case of the two-cylinder model (as in eq. (16) of ref. 5) yields equations (139) and (140):

$$Q_1 = 2(1-\nu_2)\frac{\mu_1\mu_2}{\mu_0} g_1'(x)$$

$$Q_1 = 2\frac{\mu_1\mu_2}{\tilde{\mu}_0} g_1'(x)$$

$$Q_1 = \tilde{Q}_1 \tag{139}$$

$$Q_2 = 2(1-\nu_2)\frac{\mu_1\mu_2}{\mu_0} g_2'(x)$$

$$Q_2 = 2\frac{\mu_1\mu_2}{\tilde{\mu}_0} g_2'(x)$$

$$Q_2 = \tilde{Q}_2 \tag{140}$$

The validity of the left and right sides of the SIE is thus established.

Numerical Solution

Fundamental Function of the Singular Integral Equation

The system of SIEs is derived for three concentric cylinders with two annular interface cracks. In both SIEs (eqs. (120) and (121)), the bonding stresses p and q are unknown and g_1 and g_2 are the known displacement differences. For the problem at hand, the SIEs have a simple Cauchy kernel and lengthy Fredholm kernels, and it is most convenient to use a numerical method to obtain the solution. Numerical solution methods for SIEs have been studied quite extensively (see refs. 8 to 12). There are two methods that have been commonly used to solve the integral equations with Cauchy-type singularities. These are the quadrature method and the series expansion method. In this study, the series expansion method is adopted (see refs. 9, 12, and 13).

Normalization of the interval of the integrals in the SIEs (eqs. (120) and (121)) yields equations (141) and (142):

$$-\gamma^* q(s) - \frac{1}{\pi}\int_{-1}^{1} \frac{p(\xi)}{\xi - s} d\xi - \frac{1}{\pi}\int_{-1}^{1} \left[k_{11}(s,\xi)p(\xi) + k_{12}(s,\xi)q(\xi)\right] d\xi = Q_1(s) \tag{141}$$

$$\gamma^* p(s) - \frac{1}{\pi}\int_{-1}^{1} \frac{q(\xi)}{\xi - s} d\xi + \frac{1}{\pi}\int_{-1}^{1} \left[k_{21}(s,\xi)p(\xi) + k_{22}(s,\xi)q(\xi)\right] d\xi = Q_2(s) \tag{142}$$

The system of SIEs in equations (141) and (142) can be written as one complex equation. Multiplying equation (141) by $-i$ and adding the result to the second equation (142) yields the single SIE in equation (143), with the terms defined in equations (144), (145), (146), and (147):

$$\gamma^* \phi_1(s) - \frac{1}{\pi}\int_{-1}^{1} \frac{\phi_1(\xi)}{\xi - s} d\xi + \frac{1}{2\pi}\int_{-1}^{1} \left[\hat{K}_1(s,\xi)\phi_1(\xi) + \hat{K}_2(s,\xi)\phi_2(\xi)\right] d\xi = Q(s) \tag{143}$$

$$\phi_1(s) = p(s) + iq(s) \qquad \phi_1(\xi) = p(\xi) + iq(\xi) \qquad \phi_2(\xi) = p(\xi) - iq(\xi) \tag{144}$$

$$Q(s) = Q_2(s) + iQ_1(s) \tag{145}$$

$$\hat{K}_1(s,\xi) = \frac{1}{2}\left[k_{21}(s,\xi) + k_{12}(s,\xi)\right] + i\left[k_{22}(s,\xi) + k_{11}(s,\xi)\right] \tag{146}$$

$$\hat{K}_2(s,\xi) = \frac{1}{2}\left[k_{21}(s,\xi) - k_{12}(s,\xi)\right] - i\left[k_{22}(s,\xi) - k_{11}(s,\xi)\right] \tag{147}$$

The kernels $\hat{K}_1$ and $\hat{K}_2$ are bounded and ϕ, $\hat{K}_1(s,\xi)$, $\hat{K}_2(s,\xi)$, $Q(s)$ are complex functions. The singular behavior of the function $\phi(\xi)$ at ± 1 is determined by the dominant part of the SIE. The function $\phi(\xi)$ satisfies a Holder condition on every closed subinterval of (–1, 1). Its behavior near the ends can be represented by equation (148):

$$\phi(s) = w(s)f(s) \qquad |s| < 1 \tag{148}$$

The function f is Holder-continuous on any closed subinterval of (–1, 1). This means that $p(s)$ and $q(s)$ are continuous on the open interval $-1 < s < 1$ and that $\phi(\xi)$ has integrable singularities at $s \pm 1$. The Fredholm kernels are also Holder-continuous with respect to both variables along the integration interval. The dominant part of the SIE is considered to be equal to zero so that the fundamental function can be

found. The fundamental function $w(s)$ is obtained from the homogeneous dominant part given by equation (149):

$$-\frac{1}{\pi i}\int_{-1}^{1}\frac{w(s)}{s-\xi}d\xi+\gamma^{*}w(s)=0 \tag{149}$$

The fundamental function $w(s)$ in equation (149) can be expressed as in equation (150) (ref. 13):

$$w(s)=(1-s)^{\lambda}(1+s)^{\beta} \tag{150}$$

where λ and β are defined in equations (151) and (152):

$$\lambda=-\frac{1}{2}-i\,\overline{\omega} \tag{151}$$

$$\beta=-\frac{1}{2}+i\,\overline{\omega} \tag{152}$$

The term $\overline{\omega}$ in equations (151) and (152) is defined in equation (153):

$$\overline{\omega}=\frac{1}{2\pi}\log\left(\frac{1+\gamma^{*}}{1-\gamma^{*}}\right) \tag{153}$$

The boundaries for the real part of λ and β in equations (151) and (152) are defined in equation (154):

$$\begin{aligned}-1<Re\,\lambda<0\\ -1<Re\,\beta<0\end{aligned} \tag{154}$$

In equation (150), $w(s)$ is the weight function that depends on the index of the singularities. The index of the singularity κ for a given problem is defined in equation (155):

$$\begin{gathered}\kappa=-(\lambda+\beta)\\ \kappa=-\left[\left(-\frac{1}{2}-i\overline{\omega}\right)+\left(-\frac{1}{2}+i\overline{\omega}\right)\right]\\ \kappa=1\end{gathered} \tag{155}$$

Solution by Jacobi Polynomials

After the fundamental function $w(s)$ of the SIE is obtained, the solution of equation (143) becomes equation (156):

$$\phi(s)=\sum_{0}^{\infty}\hat{c}_n w(s)P_n^{(\lambda,\beta)}(s) \tag{156}$$

In equation (156), $\hat{c}_n$ are defined as undetermined constants that need to be calculated with $n = 0, 1, \ldots$. The term $P_n^{(\lambda,\beta)}(s)$ is the Jacobi polynomial. The fundamental function $w(s)$ of the SIE in equation (156) is the weight function of the Jacobi polynomials. The details of the procedure considered here are studied extensively in references 9, 12, 13, and 14.

Substituting equation (156) into equation (143) yields equation (157) (ref. 9):

$$\frac{1}{\pi}\int_{-1}^{1} w(s)P_n^{(\lambda,\beta)}(s)\frac{ds}{s-\xi} = -\frac{\gamma^*}{(-i)}w(s)P_n^{(\lambda,\beta)}(s) - \frac{2^{-1}\Gamma(\alpha)\Gamma(1-\alpha)}{\pi}P_{n-1}^{(-\lambda,-\beta)}(s) \qquad (|s|)<1 \qquad (157)$$

The SIE (157) becomes equation (158). The terms in equation (158) are defined in equations (159), (160), and (161):

$$\sum_{0}^{\infty}\left\{\hat{c}_n\left[-\frac{2^{-1}}{i\sin(\pi\lambda)}P_{n-1}^{(-\lambda,-\beta)}(s)+h_n(s)\right]+\bar{\hat{c}}_n h_n^*(s)\right\} = Q(s) \qquad (158)$$

$$h_n(s) = \int_{-1}^{1} w(\xi)P_n^{(\lambda,\beta)}(\xi)\hat{K}_1(s,\xi)d\xi \qquad (159)$$

$$h_n^*(s) = \int_{-1}^{1} \overline{w}(\xi)\overline{P}_n^{(\lambda,\beta)}(\xi)\hat{K}_2(s,\xi)d\xi \qquad (-1<s<1) \qquad (160)$$

$$\overline{w}(\xi)\overline{P}_n^{(\alpha,\beta)}(\xi) \qquad (161)$$

where (ξ) is the conjugate of $w(\xi)P_n^{(\alpha,\beta)}(\xi)$.

In equation (158), $\bar{\hat{c}}$ is the conjugate of $\hat{c}$. So that the functional equation (158) can be reduced to an infinite system of algebraic equations with the unknown coefficients c_n, both sides of the equation are multiplied by $w(-\lambda,-\beta,s)P_m^{(-\lambda,-\beta)}(s)$ with $(m = 0, 1, 2, \ldots)$ and are integrated over (–1, 1). The orthogonality relation of the Jacobi polynomials in equation (162) is also used:

$$\int_{-1}^{1} w(s)P_n^{(\lambda,\beta)}(s)P_m^{(\lambda,\beta)}(s)ds = \begin{cases} 0, & n \neq m; \quad n,m = 0,1,2,\ldots \\ \theta_m^{(\lambda,\beta)} = \dfrac{2^{\lambda+\beta+1}}{2m+\alpha+\beta+1}\dfrac{\Gamma(m+\lambda+1)\Gamma(m+\beta+1)}{m!\Gamma(m+\lambda+\beta+1)} & n = m \end{cases} \qquad (162)$$

Since the index of the singularity is $\kappa = 1$ for $m = 0$, the right side of equation (162) becomes equation (163), with the Jacobi polynomial defined in equation (164):

$$\theta_0^{(\lambda,\beta)} = \int_{-1}^{1} w(s)ds = \frac{2^{\lambda+\beta+1}\Gamma(\lambda+1)\Gamma(\beta+1)}{\Gamma(\lambda+\beta+2)} \qquad (163)$$

$$P_0^{(\lambda,\beta)}(s) = 1.0 \qquad (164)$$

Truncating the series of equation (158) for the first N terms yields equation (165):

$$-\frac{2^{-1}}{\sin(\pi\lambda)}\theta_m(-\lambda,-\beta)\hat{c}_{m+1}+\sum_{n=0}^{N}\left(d_{nm}\hat{c}_n+d_{nm}^{*}\bar{\hat{c}}_n\right)=T_m \quad (m=0,1,\ldots,N) \tag{165}$$

Terms in equation (165) are defined in equations (166) to (172):

$$\hat{c}_{m+1}=\hat{C}R_{m+1}+i\hat{C}I_{m+1} \tag{166}$$

$$\hat{c}_n=\hat{C}R_n+i\hat{C}I_n \tag{167}$$

$$\bar{\hat{c}}_n=\hat{C}R_n-i\hat{C}I_n \tag{168}$$

$$d_{nm}=\int_{-1}^{1}P_m^{(-\lambda,-\beta)}(s)w(-\lambda,-\beta,s)h_n(s)ds \tag{169}$$

$$d_{nm}^{*}=\int_{-1}^{1}P_m^{(-\lambda,-\beta)}(s)w(-\lambda,-\beta,s)h_n^{*}(s)ds \tag{170}$$

$$T_m=\int_{-1}^{1}P_m^{(-\lambda,-\beta)}(s)w(-\lambda,-\beta,s)Q(s)ds \tag{171}$$

$$w(-\lambda,-\beta,s)=(1-s)^{-\lambda}(1+s)^{-\beta}=w^{-1}(s) \tag{172}$$

The matrix form of equation (165) is written in equation (173):

$$\left[A^{*}\right]_{2(N+1),2(N+2)}\begin{Bmatrix}\hat{C}R\\ \hat{C}I\end{Bmatrix}_{2(N+2)}=\begin{Bmatrix}TR\\ TI\end{Bmatrix}_{2(N+2)} \tag{173}$$

where

$\hat{C}R$	real part of $\hat{c}$
$\hat{C}I$	imaginary part of $\hat{c}$
TR	real part of the right side
TI	imaginary part of the right side

The number of equations in equation (173) is $2(N + 1)$. There are $2(N + 2)$ unknown constants: $\hat{C}R_0$, $\hat{C}R_1$, $\hat{C}R_{N+1}$ and $\hat{C}I_0$, $\hat{C}I_1$, and $\hat{C}I_{N+1}$. Therefore, the continuity condition is the additional equation used to provide the unique solution given in equation (174):

$$\int_{-1}^{1}\phi(s)ds=0 \tag{174}$$

Substituting equation (156) into equation (174) and using the orthogonality conditions in equation (162) yields equation (175):

$$\left(\hat{C}R + i\hat{C}I\right)\theta_0(\lambda,\beta) = 0 \tag{175}$$

Adding an additional equation (eq. (175)) into equation (173) yields equation (176):

$$[A]_{2(N+2),2(N+2)}\begin{Bmatrix}\hat{C}R\\ \hat{C}I\end{Bmatrix}_{2(N+2)} = \begin{Bmatrix}TR\\ TI\end{Bmatrix}_{2(N+2)} \tag{176}$$

Any standard method of solution of the system of algebraic equations can be used to determine the unknown $\hat{c}$ in terms of $\hat{C}R$ and $\hat{C}I$, as in equation (177):

$$\begin{Bmatrix}\hat{C}R\\ \hat{C}I\end{Bmatrix}_{2(N+2)} = [A]^{-1}_{2(N+2),2(N+2)}\begin{Bmatrix}TR\\ TI\end{Bmatrix}_{2(N+2)} \tag{177}$$

From equation (177), the unknown constants $\hat{C}R_0,\ \hat{C}R_1,\ \ldots,\ \hat{C}R_{N+1}$ and $\hat{C}I_0,\ \hat{C}I_1,\ \ldots,\ \hat{C}I_{N+1}$, are known. These constants determine $\hat{c}_0,\ \hat{c}_1,\ \ldots,\ \hat{c}_{N+1}$, which are defined in equation (178):

$$\begin{aligned}\hat{c}_0 &= \hat{C}r_0 + i\hat{C}I_0\\ \hat{c}_1 &= \hat{C}r_1 + i\hat{C}I_1\\ &\vdots\\ \hat{c}_{N+1} &= \hat{C}R_{N+1} + i\hat{C}I_{N+1}\end{aligned} \tag{178}$$

Gauss-Jacobi Quadrature Technique

The objective of the numerical work in this technique involves the evaluation of the unknown constants. However, since the related integrals are of the Gauss-Jacobi type, these constants may be evaluated accurately without computational difficulty (ref. 9). The quadrate formula, which can be used for this purpose, is defined in equation (179) (ref. 15).

$$T(s) = \int_{-1}^{1}(1-s)^{-\lambda}(1+s)^{-\beta} f(s)ds \cong \sum_{k=1}^{N}\Omega_m f(s_m) \tag{179}$$

where s_k and $m = 1, \ldots, N$ are the roots of the orthogonal polynomial $P_N^{(-\lambda,-\beta)}(s_k) = 0$, $m = 0, \ldots, N$. The weights of equation (179) are defined in equation (180):

$$\Omega_m = -\frac{2N-\lambda-\beta+2}{(N+1)!(N-\lambda-\beta+1)}\frac{\Gamma(N-\lambda+1)\Gamma(N-\beta+1)}{\Gamma(N-\lambda-\beta+1)}\frac{2^{-\lambda-\beta}}{P_N^{'(-\lambda,-\beta)}(s_m)P_{N+1}^{(-\lambda,-\beta)}(s_m)} \tag{180}$$

$$h_n(s_m) = \int_{-1}^{1} (1-\xi)^{\lambda}(1+\xi)^{\beta} f(s_m,\xi)d\xi \cong \sum_{n=1}^{N} \hat{\Omega}_n f(s_m,\xi_n) \tag{181}$$

where ξ_n, $n = 1, \ldots, N$, are the roots of $P_N^{(\alpha,\beta)}(\xi_n) = 0$. The weights of equation (181) are defined in equation (182):

$$\hat{\Omega}_n = -\frac{2N+\lambda+\beta+2}{(N+1)!(N+\lambda+\beta+1)} \frac{\Gamma(N+\lambda+1)\Gamma(N+\beta+1)}{\Gamma(N+\lambda+\beta+1)} \frac{2^{\lambda+\beta}}{P_N'^{(\lambda,\beta)}(\xi_n)P_{N+1}^{(\lambda,\beta)}(\xi_n)} \tag{182}$$

Stress Intensity Factor

In the immediate neighborhood of the crack tips, the form of the solution is identical to that of the plane strain, and the bonding stresses may be expressed as in equation (183) (ref. 5):

$$p(x) + iq(x) \cong p_0\left(\Re_1(x) + i\Re_2(x)\right)\frac{\sin\tau - i\cos\tau}{\sqrt{(1-x^2)}}$$

$$\tau = \overline{\omega}\log\left(\frac{1+x}{1-x}\right)$$

$$\overline{\omega} = \frac{1}{2\pi}\log\left(\frac{1+\gamma^*}{1-\gamma^*}\right) \quad (-1 < x < 1) \tag{183}$$

where the bounded functions $\Re_1$ and $\Re_2$ are the intensities of stresses and are proportional to the external loads.

Also from the formulation of the problem, the equation $\phi(x) = p(x) + iq(x)$ can be written as in equation (184):

$$\phi(x) = \sum_{i=1}^{N} \hat{c}_i w(x) P_N^{(\lambda,\beta)}(x) \tag{184}$$

In equation (184), the fundamental function $w(x)$ is defined in equation (185):

$$w(x) = (1-x)^{-(1/2)-i\overline{\omega}}(1+x)^{-(1/2)+i\overline{\omega}} \tag{185}$$

The term in equation (185) is defined in equation (186):

$$\overline{\omega} = \frac{1}{2\pi}\log\left(\frac{1+\gamma^*}{1-\gamma^*}\right) \tag{186}$$

Therefore, equation (186) becomes equation (187):

$$w(x) = \left(1-x^2\right)^{-\frac{1}{2}}\left(\frac{1+x}{1-x}\right)^{i\overline{\omega}} \tag{187}$$

Equation (187) can be written in different forms, as defined in equations (188) to (190):

$$w(x) = \frac{1}{\sqrt{1-x^2}} e^{i\bar{\omega}\log\left(\frac{1+x}{1-x}\right)} \tag{188}$$

$$w(x) = \frac{e^{i\tau}}{\sqrt{1-x^2}} \tag{189}$$

or

$$w(x) = \frac{\cos\tau + i\sin\tau}{\sqrt{1-x^2}} \tag{190}$$

This last form of the fundamental function (eq. (190)) is multiplied by i/i and uses $1/i = -i$. The fundamental function in equation (190) is rewritten in equation (191):

$$\begin{aligned} w(x) &= \frac{i}{i}\frac{\cos\tau + i\sin\tau}{\sqrt{1-x^2}} \\ w(x) &= \frac{1}{i}\frac{(-\sin\tau + i\cos\tau)}{\sqrt{1-x^2}} \\ w(x) &= i\frac{\sin\tau - i\cos\tau}{\sqrt{1-x^2}} \end{aligned} \tag{191}$$

Substituting equations (184) and (191) into equation (183) yields equation (192):

$$\sum_{n=0}^{N}\left[i\hat{c}_n P_N^{(\lambda,\beta)}(x)\right]\frac{\sin\tau - i\cos\tau}{\sqrt{\left(1-x^2\right)}} \cong p_0\left[\Re_1(x) + i\Re_2(x)\right]\frac{\sin\tau - i\cos\tau}{\sqrt{\left(1-x^2\right)}} \tag{192}$$

After necessary simplifications are made, equation (192) becomes equation (193):

$$p_0\left[\Re_1(x) + i\Re_2(x)\right] \cong \sum_{n=0}^{N}\left[i\hat{c}_n P_N^{(\lambda,\beta)}(x)\right] \tag{193}$$

It can be shown that (ref. 16), in terms of $\phi(x)$, the bonding stresses in the neighborhood of the crack tip may be expressed as in equation (194):

$$\begin{aligned} \sigma_r - i\tau_{rx} &= p(x) + iq(x) \\ \sigma_r - i\tau_{rx} &= p_0\left[\Re_1(x) + i\Re_2(x)\right]\frac{\sin\tau - i\cos\tau}{\sqrt{1-x^2}} \\ r &= r_c \quad |x| < 1 \end{aligned} \tag{194}$$

Thus, the stress intensity (ref. 5) is defined as

$$\sigma_r - i\tau_{rx} = \left(\hat{k}_1 - i\hat{k}_2\right)\frac{\sin\tau - i\cos\tau}{\sqrt{1-x^2}} \tag{195}$$

where $-1 < x < 1$. Since the left side of equations (194) and (195) are the same, the right side of equations (194) and (195) are equal to each other. Therefore, the SIFs are obtained as in equation (196):

$$\begin{aligned}
\hat{k}_1(a) &= p_0\Re_1(a) \\
\hat{k}_1(b) &= p_0\Re_1(b) \\
\hat{k}_2(a) &= -p_0\Re_2(a) \\
\hat{k}_2(b) &= -p_0\Re_2(b)
\end{aligned} \tag{196}$$

Strain Energy Release Rate

The SERRs for modes I and II for a crack along the interface may be expressed as in reference 5:

$$\begin{aligned}
G_1(a) &= \frac{\pi}{2}\frac{\left(\mu_1+\kappa_1\mu_3\right)\left(\mu_3+\kappa_3\mu_1\right)}{\mu_1\mu_3\left[\left(1+\kappa_3\right)\mu_1+\left(1+\kappa_1\right)\mu_3\right]}\hat{k}_1^2(a) \\
G_1(b) &= \frac{\pi}{2}\frac{\left(\mu_1+\kappa_1\mu_3\right)\left(\mu_3+\kappa_3\mu_1\right)}{\mu_1\mu_3\left[\left(1+\kappa_3\right)\mu_1+\left(1+\kappa_1\right)\mu_3\right]}\hat{k}_1^2(b) \\
G_2(a) &= \frac{\pi}{2}\frac{\left(\mu_1+\kappa_1\mu_3\right)\left(\mu_3+\kappa_3\mu_1\right)}{\mu_1\mu_3\left[\left(1+\kappa_3\right)\mu_1+\left(1+\kappa_1\right)\mu_3\right]}\hat{k}_2^2(a) \\
G_2(b) &= \frac{\pi}{2}\frac{\left(\mu_1+\kappa_1\mu_3\right)\left(\mu_3+\kappa_3\mu_1\right)}{\mu_1\mu_3\left[\left(1+\kappa_3\right)\mu_1+\left(1+\kappa_1\right)\mu_3\right]}\hat{k}_2^2(b)
\end{aligned} \tag{197}$$

The total SERR is then obtained as

$$\begin{aligned}
\frac{\partial U(a)}{\partial c} &= G(a) = \left[\hat{k}_1^2(a)+\hat{k}_2^2(a)\right]\frac{\pi}{2}\frac{\left(\mu_1+\kappa_1\mu_3\right)\left(\mu_3+\kappa_3\mu_1\right)}{\mu_1\mu_3\left[\left(1+\kappa_3\right)\mu_1+\left(1+\kappa_1\right)\mu_3\right]} \\
\frac{\partial U(b)}{\partial c} &= G(b) = \left[\hat{k}_1^2(b)+\hat{k}_2^2(b)\right]\frac{\pi}{2}\frac{\left(\mu_1+\kappa_1\mu_3\right)\left(\mu_3+\kappa_3\mu_1\right)}{\mu_1\mu_3\left[\left(1+\kappa_3\right)\mu_1+\left(1+\kappa_1\right)\mu_3\right]}
\end{aligned} \tag{198}$$

Application of the Method

As an illustration of the use of the numerical approach developed in this report, the sensitivity of the SERR and SIF to coating stiffness and thickness are examined using material properties representative of polymer matrix composites. The method is applied to the case of a single fiber embedded in an infinite matrix with a radial load applied to the matrix. In the SIE, Q_1 and Q_2 are functions of closed displacement differences that are related to the applied load at infinity:

$$Q_1 = 2(1-\nu_3)\frac{\mu_1\mu_3}{\mu_0}g_1'(x)$$

$$Q_2 = 2(1-\nu_3)\frac{\mu_1\mu_3}{\mu_0}g_2'(x) \tag{199}$$

The displacement differences that are assumed to be known are associated with an elasticity solution. So that the solutions can be found, two different cylinders must be formed. The first is a hollow outer cylinder that represents the matrix. This cylinder has an infinite outer radius. Since the fiber and coating are considered to be perfectly bonded, the second cylinder is a solid cylinder formed by combining the inner solid cylinder (fiber) with the middle hollow cylinder (coating). There is no bond between the two cylinders, and external loads are applied separately to the two cylinders.

In the example that is considered here, the external radial stress $\sigma_{r1}(\infty, x) = \sigma_0 = 1$ lb/in.^{2} is applied to the outer (matrix) cylinder. Index r is for the radial direction, and index 1 is for the matrix. There is no load applied to the second cylinder. Then, from the elasticity solution of the problem, the surface displacements for the first cylinder (matrix) and the second cylinder (coating and fiber) are

$$u_{r1} = \frac{2\sigma_0 r}{E_1}$$

$$u_{x1} = -\frac{2\sigma_0\nu_1}{E_1}x$$

$$u_{r3} = u_{x3} = 0 \tag{200}$$

The displacement differences that need to be closed at the matrix-coating (region 1 to region 3) interface can be written as

$$-(u_{r1} - u_{r3}) = g_1(x)$$

$$-(u_{x1} - u_{x3}) = g_2(x) \tag{201}$$

where $r = r_c$ and $x \in L$. Therefore, rewriting equations in equation (201) yields

$$g_1(x) = -\frac{2\sigma_0 r_c}{E_1}$$

$$g_2(x) = \frac{2\sigma_0\nu_1}{E_1}x \tag{202}$$

As an example, symmetric loading and a single bond are considered where $L = (-1, 1)$ and L' is infinitely long. For the SIE, a zero stress state at infinity is solved; Q_1 and Q_2 are the only loadings that are considered. In the SIE, $g_1(x)$ and $g_2(x)$ are expressed as

$$g_1(x) = -2\beta_1\frac{\mu_0}{(1-\nu_3)\mu_1\mu_3}$$

$$g_2(x) = 2\beta_2\frac{\mu_0}{(1-\nu_3)\mu_1\mu_3}x \tag{203}$$

Equations (202) and (203) are used to find β_1 and β_2 as in equation (204):

$$\beta_1 = \frac{4(1-\nu_3)\mu_1\mu_3\sigma_0 r_c}{\mu_0 E_1}$$
$$\beta_2 = \frac{4(1-\nu_3)\mu_1\mu_3\sigma_0\nu_1}{\mu_0 E_1} \tag{204}$$

Substituting equations (203) and (204) into equation (199) yields equation (205):

$$Q_1(x) = 0$$
$$Q_2(x) = \beta_2$$
$$Q_2(x) = \frac{4(1-\nu_3)\mu_1\mu_3\sigma_0\nu_1}{\mu_0 E_1} \tag{205}$$

The effects of material properties and crack size on the SERR are now considered. In the SIE, the integrals from –1 to 1 that contain Jacobi polynomials are taken by using the Gauss-Jacobi quadrature technique. Providing an adequate number of points is important for convergence. As shown in figure 5, convergence begins at about 16 points. The material properties used here are the same as those used in reference 5. The material properties of the matrix (indicated by a subscript 1) are $E_1 = 4.5\times10^5$ lb/in.^{2} and $\nu_1 = 0.35$, and the properties of the fiber (indicated by a subscript 2) are $E_2 = 10^7$ lb/in.^{2} and $\nu_2 = 0.2$.

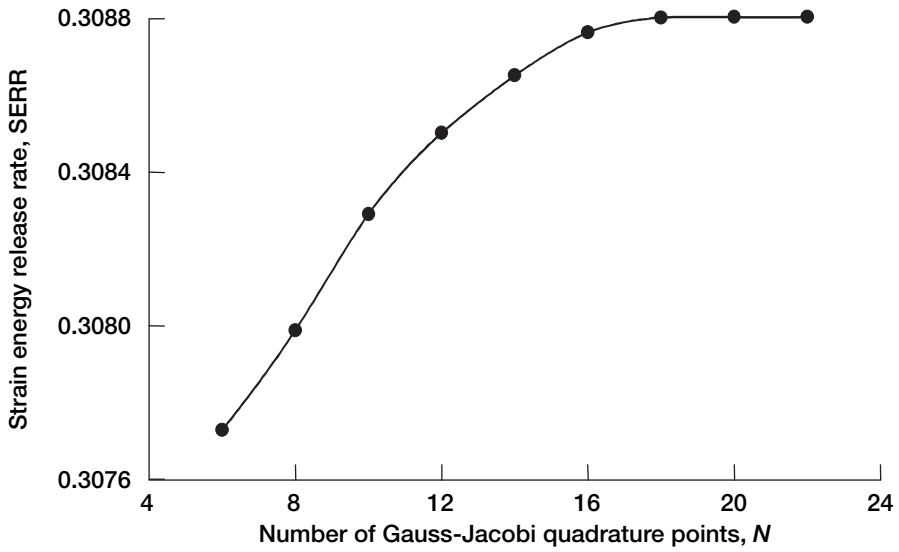

Figure 5.—Number of Gauss-Jacobi quadrature points.

The radius of the coating is 1, and the radius of the fiber is 0.5. In this example, the value of $\nu_3 = 0.2$ is not changed, but E_3 ranges from E_1 to E_2 and from E_2 to $E = 10^8$ lb/in.^{2} The parametric studies are presented for the normalized mode-I and mode-II SIF: that is, equation (206) with $c = L/2$, and a normalized SERR; in other words, equation (209), which is derived from equations (207) and (208):

$$\frac{\hat{k}_1}{\sigma_0\sqrt{c}} \quad \frac{\hat{k}_2}{\sigma_0\sqrt{c}} \tag{206}$$

$$G = (\hat{k}_1^2 + \hat{k}_2^2)\frac{\pi}{2}\frac{(\mu_1 + K_1\mu_3)(\mu_3 + K_3\mu_1)}{\mu_1\mu_3\left[(1+K_1)\mu_3 + (1+K_3)\mu_1\right]} \tag{207}$$

$$G_0 = \frac{\pi}{2}\frac{(\mu_1 + K_1\mu_3)(\mu_3 + K_3\mu_1)}{\mu_1\mu_3\left[(1+K_1)\mu_3 + (1+K_3)\mu_1\right]} \tag{208}$$

$$\frac{G}{G_0} = \hat{k}_1^2 + \hat{k}_2^2 \tag{209}$$

In figure 6, the SERR and SIF are plotted versus coating stiffness E_3 with a lower bound equal to the matrix stiffness E_1 and an upper bound equal to the fiber stiffness E_2: that is, $E_1 = 4.5\times10^5 \le E_3 \le E_2 = 10^7$. The SERR and SIF are sensitive to variations in coating stiffness when the coating stiffness is close to the matrix stiffness. As the coating stiffness increases, the SERR increases and becomes less sensitive to variations in coating thickness. Figure 7 is similar to figure 6 except that the maximum coating stiffness (10^8) is 10 times the fiber stiffness. The SERR and SIF are nearly independent of coating stiffness when the coating stiffness exceeds the fiber stiffness. For polymer matrix composites, these results suggest that the driving force for crack growth will be sensitive to the stiffness of the interphase and that the driving force will increase significantly as the stiffness of the interphase increases beyond the stiffness of the matrix. For the hypothetical case in which interphase stiffness changes but the critical SERR for crack propagation remains constant, an increase in the stiffness of the interphase would result in crack propagation at a lower applied load.

The effect of coating thickness on the SERR and SIF is shown in figure 8. The material properties used to obtain the data in figure 8 are $E_1 = 4.5\times10^5$ lb/in.^{2}, $\nu_1 = 0.35$ for the matrix; $E_2 = 10^7$ lb/in.^{2}, $\nu_2 = 0.2$ for the fiber; and $E_3 = 10^8$ lb/in.^{2}, $\nu_3 = 0.2$ for the coating. The ratio of the coating thickness to half of the bonded length (h_3/c) is varied from 0.05 to 2. The normalized SERR and SIF versus the ratio h_3/c is shown in figure 8. Since the SERR increases with increasing coating thickness, coating thickness could result in crack propagation at a lower applied load. This conclusion is valid only if the critical SERR is not affected by the coating thickness. In addition, this conclusion applies only for the material properties assumed in the analysis. In this analysis, the coating stiffness was greater than the fiber stiffness. A different analysis would be needed to evaluate the effect of interphase thickness in a material system in which the interphase stiffness is closer to the matrix stiffness.

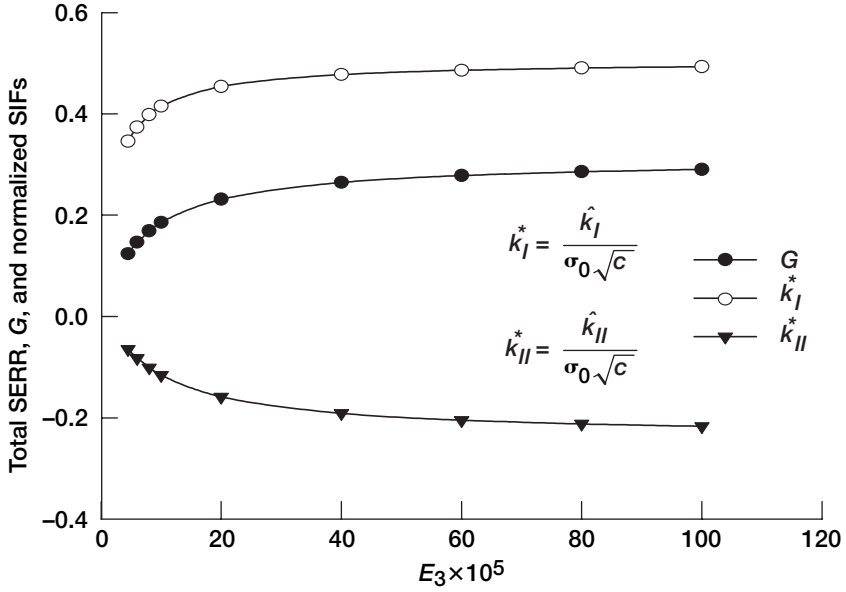

Figure 6.—Stress intensity factors (SIFs) and strain energy release rate (SERR) versus $E_3\times10^5$ ranging from $E_1 = 4.5\times10^5$ to $E_2 = 10^7$ where c is half the bounded length ($c = L/2$).

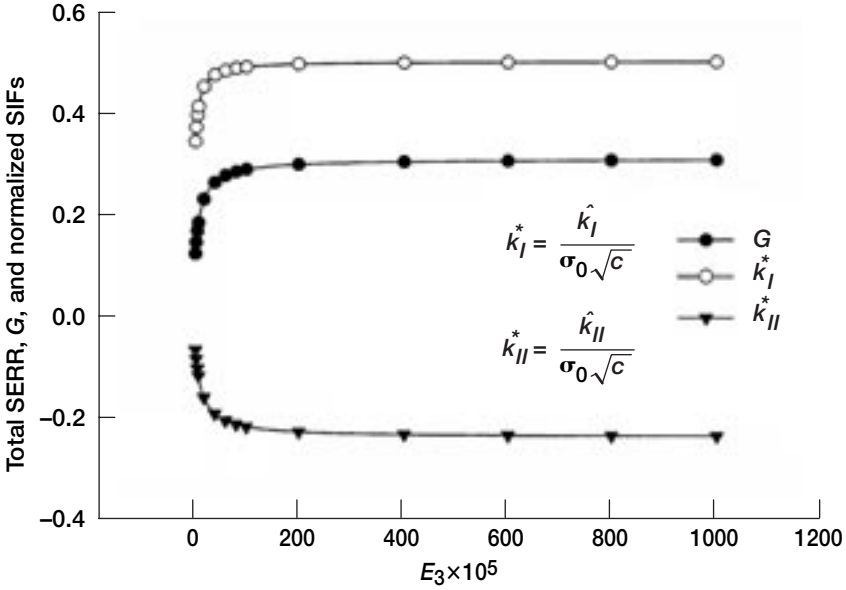

Figure 7.—Stress intensity factors (SIFs) and strain energy release rate (SERR) versus $E_3\times10^5$ ranging from $E_1 = 8\times10^6$ to $E_2 = 10^8$.

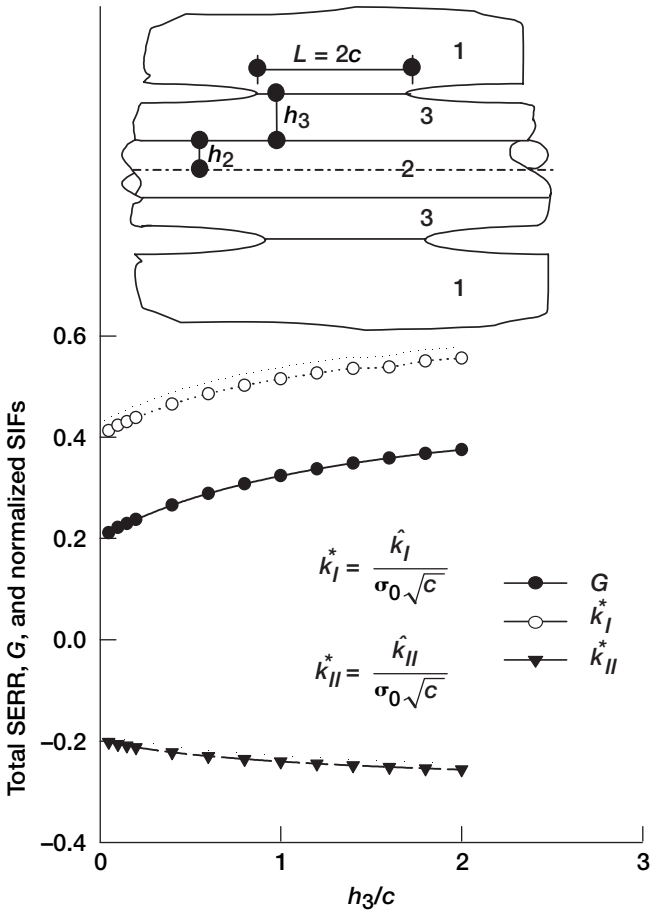

Figure 8.—Stress intensity factors (SIFs) and strain energy release rate (SERR) versus h_3/c for $h_2 = 0.2$.

Conclusions

An analytical model was developed to calculate the SIF and SERR for an infinitely long straight fiber and an infinite matrix that were partly joined using a third material called the interphase (or coating). The addition of a third (interphase) region is an extension of a two-component model previously described in reference 5. The ability to evaluate the effect of interphase geometry and material properties makes the model more realistic for polymer matrix composites, which are known to have an interphase region. A preliminary set of parametric studies demonstrated the effect of interphase properties on the SERR. An advantage of this analytical method is that calculation of the SERR and SIF is straightforward for problems with cylindrical symmetry. Although cylindrical symmetry does not necessarily apply in a real composite structure, the method is still useful as a simple tool to provide insight about the effect of interphase properties on the crack driving force. The model can also be applied to other material systems such as ceramic or metal matrix composites by using the appropriate material properties. Further development of the method to account for different loading conditions and different crack types would make the method even more useful, particularly for experiments such as fiber pullout or growth of a debond area in a single fiber test where the SIF and SERR solutions are still lacking.

Appendix—Symbols

A_1, B_1, C_1, D_1	unknown constants for layer 1 (matrix)
A_2, B_2, C_2, D_2	unknown constants for layer 2 (fiber)
A_3, B_3, C_3, D_3	unknown constants for layer 3 (coating)
C	half of the bounded length
E_1, E_2, E_3	modulus of elasticity for the matrix, fiber, and coating
F	Love strain function or Green's function
F_1, F_2, F_3	Green's functions for the matrix, fiber, and coating, respectively
g_1, g_2	known displacement gaps along the 1 and 2 directions
$G_1(a), G_1(b), G_2(a), G_2(b)$	strain energy release rates (SERRs)
I_0, I_1, K_0, K_1	modified Bessel functions of order 0 and 1, respectively
$k_{\mathrm{I}}^*,\ k_{\mathrm{II}}^*$	normalized stress intensity factors for modes I and II
$\hat{k}_1(a), \hat{k}_1(b), \hat{k}_2(a), \hat{k}_2(b)$	stress intensity factors (SIFs)
L	length of the bonded interface
L'	length of the debonded interface
$P_N^{(-\lambda,-\beta)}(s_k)$	Jacobi polynomial
p, q	unknown stresses outside the crack, on the bonded interface
Q_1, Q_2	functions of closed displacement differences along the radial and axial directions
Re	real part of a complex number
$\Re_1, \Re_2$	stress intensities
r	radial distance
r_c	coating radius
r_f	fiber radius
r_m	matrix radius
s	dummy variable
t	dummy variable of the Fourier domain
u_r, u_x	displacements along the r and x directions, respectively
$w(x)$	fundamental function
x	axial distance
α	$r_c t$, where $r_1 = r_2 = r_c$
Γ	gamma function
γ	$r_f t$, where $r_2 = r_3 = r_f$
γ^*	material parameter
δ	Dirac delta function
θ	cylindrical coordinate
κ	index of the singularity
$(\mu_1,\nu_1),(\mu_2,\nu_2),(\mu_3,\nu_3)$	elastic constants of the matrix, fiber, and coating, respectively
ν	Poisson's ratio
ξ	dummy variable
ρ	variable (a function of rt)
$\sigma_r,\sigma_\theta,\sigma_\xi$	stresses along the r-, θ-, and x-axis, respectively
τ_{rx}	shear stresses along the r-x direction

ϕ	complex form of the unknown stresses outside the crack, on the bounded interface
∇^2	Laplacian operator in cylindrical coordinates

Subscripts:

1 or *m*	related to the matrix
2 or *f*	related to the fiber
3 or *c*	related to the coating

References

1. Sih, G.C.; and Skudra, A.M.: Failure Mechanics of Composites. Elsevier Science Publishing Co., Amsterdam, 1985.
2. Liebowitz, Harold: Fracture, An Advanced Treatise. Academic Press, New York, NY, 1968.
3. Yang, F.; and Pitchumani, R.: Modeling of Interphase Formation on Unsized Fibers in Thermosetting Composites. Proceedings of the ASME Heat Transfer Division, vol. 3, ASME–HTD–Vol. 366–3, 2000, pp. 329–337.
4. Bogetti, T.A., et al.: Characterization of Nanoscale Property Variations in Polymer Composite Systems: 2. Numerical Modeling. CPSOA, vol. 30A, no. 1, 1999, pp. 85–94.
5. Özbek, T.; and Erdogan, F.: Some Elasticity Problems in Fiber-Reinforced Composites With Imperfect Bonds. Int. J. Engrg. Sci., vol. 7, 1969, pp. 931–946.
6. Erdogan, F.; and Özbek, T.: Stresses in Fiber-Reinforced Composites With Imperfect Bonding. J. Appl. Phys., 1969, pp. 865–869.
7. Timoshenko, S.; and Goodier, J.N.: Theory of Elasticity. McGraw-Hill, New York, 1951.
8. Muskhelishvili, Nikolaei Ivanovich: Singular Integral Equations; Boundary Problems of Function Theory and Their Application to Mathematical Physics. Noordhoff, Groningen, 1953.
9. Erdogan, F.; Gupta, G.D.; and Cook, T.S.: Numerical Solution of Singular Integral Equations. Methods of Analysis and Solutions of Crack Problems—Recent Developments in Fracture Mechanics. Theory and Methods of Solving Crack Problems. George C. Sih, ed., Noordhoff International Pub., Leyden, Netherlands, 1973, p. 368.
10. Krenk, Steen: On Quadrature Formulas for Singular Integral Equations of the First and the Second Kind. Q. Appl. Math., vol. XXXIII, no. 3, 1975, pp. 225–232.
11. Binienda, Wieslaw Kazimierz: Mixed-Mode Fracture in Fiber-Reinforced Composite Materials. Ph.D. Dissertation, Drexel University, 1987.
12. Erdogan, F.: Mixed Boundary Value Problems in Mechanics. NASA CR–145042, 1975.
13. Erdogan, F.; and Gupta, G.D.: Layered Composites With an Interface Flaw. Int. J. Solids Structures, vol. 7, pp. 1971, 1089–1107.
14. Kuguoglu, Latife Hamide: Analytical Modeling of Imperfect Bond Between Coated Fibers and Matrix Material. Ph.D. Dissertation, University of Akron, 1999.
15. Stroud, A.H.; and Secrest, D.: Gaussian Quadrature Formulas. Prentice-Hall, Englewood Cliffs, NJ, 1966.
16. Erdogan, Fazil: Stress Distribution in a Nonhomogeneous Elastic Plane With Cracks. J. Appl. Mech. Trans. ASME, series E, 1963, pp. 232–236.

REPORT DOCUMENTATION PAGE

Form Approved
OMB No. 0704-0188

Public reporting burden for this collection of information is estimated to average 1 hour per response, including the time for reviewing instructions, searching existing data sources, gathering and maintaining the data needed, and completing and reviewing the collection of information. Send comments regarding this burden estimate or any other aspect of this collection of information, including suggestions for reducing this burden, to Washington Headquarters Services, Directorate for Information Operations and Reports, 1215 Jefferson Davis Highway, Suite 1204, Arlington, VA 22202-4302, and to the Office of Management and Budget, Paperwork Reduction Project (0704-0188), Washington, DC 20503.

1. AGENCY USE ONLY (*Leave blank*)	2. REPORT DATE	3. REPORT TYPE AND DATES COVERED
	February 2004	Technical Memorandum

4. TITLE AND SUBTITLE

Fracture Mechanics Analysis of an Annular Crack in a Three-Concentric-Cylinder Composite Model

5. FUNDING NUMBERS

WBS–22–708–24–05

6. AUTHOR(S)

Latife H. Kuguoglu, Wieslaw K. Binienda, and Gary D. Roberts

7. PERFORMING ORGANIZATION NAME(S) AND ADDRESS(ES)

National Aeronautics and Space Administration
John H. Glenn Research Center at Lewis Field
Cleveland, Ohio 44135–3191

8. PERFORMING ORGANIZATION REPORT NUMBER

E–13923

9. SPONSORING/MONITORING AGENCY NAME(S) AND ADDRESS(ES)

National Aeronautics and Space Administration
Washington, DC 20546–0001

10. SPONSORING/MONITORING AGENCY REPORT NUMBER

NASA TM—2004-212328

11. SUPPLEMENTARY NOTES

Latife H. Kuguoglu, QSS Group, Inc., Cleveland, Ohio 44135; Wieslaw K. Binienda, University of Akron, Akron, Ohio 44325; and Gary D. Roberts, NASA Glenn Research Center. Responsible person, Gary D. Roberts, organization code 5150, 216–433–3244.

12a. DISTRIBUTION/AVAILABILITY STATEMENT

Unclassified - Unlimited
Subject Category: 64 Distribution: Nonstandard

Available electronically at http://gltrs.grc.nasa.gov

This publication is available from the NASA Center for AeroSpace Information, 301–621–0390.

12b. DISTRIBUTION CODE

13. ABSTRACT ***(Maximum 200 words)***

A boundary-value problem governing a three-phase concentric-cylinder model was analytically modeled to analyze annular interfacial crack problems with Love's strain functions in order to find the stress intensity factors (SIFs) and strain energy release rates (SERRs) at the tips of an interface crack in a nonhomogeneous medium. The complex form of a singular integral equation (SIE) of the second kind was formulated using Bessel's functions in the Fourier domain, and the SIF and total SERR were calculated using Jacoby polynomials. For the validity of the SIF equations to be established, the SIE of the three-concentric-cylinder model was reduced to the SIE for a two-concentric-cylinder model, and the results were compared with the previous results of Erdogan. A preliminary set of parametric studies was carried out to show the effect of interphase properties on the SERR. The method presented here provides insight about the effect of interphase properties on the crack driving force.

14. SUBJECT TERMS

Singular integral equations; Strain energy release rate; Fiber-matrix interfaces; Fracture mechanics; Crack propagation; Stress intensity factors; Resin matrix composites; Fiber composites

15. NUMBER OF PAGES

48

16. PRICE CODE

17. SECURITY CLASSIFICATION OF REPORT	18. SECURITY CLASSIFICATION OF THIS PAGE	19. SECURITY CLASSIFICATION OF ABSTRACT	20. LIMITATION OF ABSTRACT
Unclassified	Unclassified	Unclassified	